Molecular Therapy
Original Article

ROCK inhibition enhanced hepatocyte liver engraftment by retaining membrane CD59 and attenuating complement activation

Haoxin Ma,[1,5] Chao Wang,[1,5] Shulong Liang,[1,5] Xinlu Yu,[1] Yuan Yuan,[1] Zhuanman Lv,[1] Jiqianzhu Zhang,[2] Caixia Jin,[3] Jiangbo Zhu,[2] Chao Wang,[1] Pingxin Sun,[1] and Wenlin Li[1,4]

[1]Department of Cell Biology, Naval Medical University, Shanghai 200433, China; [2]Department of Health Toxicology, Naval Medical University, Shanghai 200433, China; [3]Department of Regenerative Medicine, College of Medicine, Tongji University, Shanghai 200433, China; [4]Shanghai Key Laboratory of Cell Engineering, Naval Medical University, Shanghai 200433, China

Hepatocyte transplantation can be an effective treatment for patients with certain liver-based metabolic disorders and liver injuries. Hepatocytes are usually infused into the portal vein, from which hepatocytes migrate into the liver and integrate into the liver parenchyma. However, early cell loss and poor liver engraftment represent major hurdles to sustaining the recovery of diseased livers after transplantation. In the present study, we found that ROCK (Rho-associated kinase) inhibitors significantly enhanced *in vivo* hepatocyte engraftment. Mechanistic studies suggested that the isolation of hepatocytes caused substantial degradation of cell membrane proteins, including the complement inhibitor CD59, probably due to shear stress-induced endocytosis. ROCK inhibition by ripasudil, a clinically used ROCK inhibitor, can protect transplanted hepatocytes by retaining cell membrane CD59 and blocking the formation of the membrane attack complex. Knockdown of CD59 in hepatocytes eliminates ROCK inhibition-enhanced hepatocyte engraftment. Ripasudil can accelerate liver repopulation of fumarylacetoacetate hydrolase-deficient mice. Our work reveals a mechanism underlying hepatocyte loss after transplantation and provides immediate strategies to enhance hepatocyte engraftment by inhibiting ROCK.

INTRODUCTION

The liver is a central organ for metabolic homeostasis. Liver disease accounts for approximately 2 million deaths per year worldwide.[1] For end-stage liver diseases, liver transplantation is the only curative treatment, but its application is limited by an inextricable shortage of donor organs and the life-long need for immunosuppression. In addition to organ transplantation, preclinical and clinical studies have also suggested that hepatocyte transplantation could be another promising strategy to treat fulminant liver diseases.[2–5] Since the first case of human hepatocyte transplantation for the treatment of liver cirrhosis in 1992,[6] there have been more than 100 clinical studies published in the literature, and hepatocyte transplantation has shown good patient tolerance and varying degrees of patient benefit.[7–9] Especially for liver metabolic diseases, hepatocyte transplantation can achieve rapid improvement of patients' clinical symptoms and even long-term disease remission.[3] For example, three rounds of hepatocyte transplants over a 5-month period for a 3.5-year-old girl with argininosuccinate lyase deficiency led to sustained metabolic and clinical control stability over a follow-up period of more than 1 year. The proportion of exogenous transplanted hepatocytes in the liver exceeded 10%.[10]

The advantage of hepatocyte transplantation over liver organ transplantation is that the surgery is less invasive, and multiple transplantations can be performed as needed. However, there are also a few major bottlenecks that impede cell therapy for liver diseases. For example, hepatocytes used in most clinical research are usually derived from livers that are not suitable for organ transplantation. The source and quality of hepatocytes severely limit the application of hepatocyte transplantation.[9] Recent progress in generating hepatocytes from stem cells or expanding hepatocytes is promising to eventually solve this issue.[11–17] Another major limitation of hepatocyte transplantation is the extremely low efficiency of hepatocyte *in vivo* engraftment. Soon after cell infusion, up to 70% of hepatocytes were lost immediately, probably due to the instant blood-mediated inflammatory reaction (IBMIR) and activation of coagulation and complement pathways, leading to subsequent hepatocyte cell death.[18–20] The surviving hepatocytes must migrate across the sinusoidal endothelial cell barrier, squeeze into liver plates, and establish cell-cell adhesion with host hepatocytes for successful engraftment. Eventually, only approximately 2%–6% of

Received 16 August 2022; accepted 23 February 2023;
https://doi.org/10.1016/j.ymthe.2023.02.018.

[5]These authors contributed equally

Correspondence: Chao Wang, Department of Cell Biology, Naval Medical University, Shanghai 200433, China.
E-mail: wangchaosmmu@126.com
Correspondence: Pingxin Sun, Department of Cell Biology, Naval Medical University, Shanghai 200433, China.
E-mail: spxcellbiology@hotmail.com
Correspondence: Wenlin Li, Department of Cell Biology, Naval Medical University, Shanghai 200433, China.
E-mail: liwenlin@smmu.edu.cn

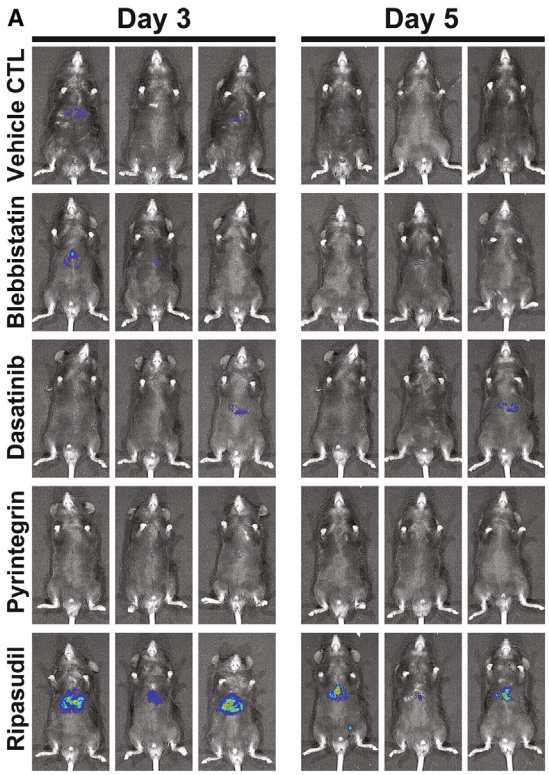

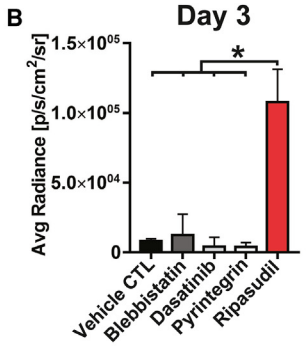

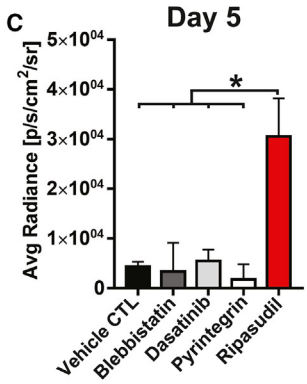

Figure 1. The ROCK inhibitor ripasudil enhances hepatocyte liver engraftment

(A) C57 mice were transplanted with luciferase-expressing hepatocytes. The effects of the ROCK inhibitor ripasudil, nonmuscle myosin II ATPase inhibitor blebbistatin, β1-integrin agonist pyrintegrin, and Src kinase inhibitor dasatinib on hepatocyte liver engraftment were analyzed by bioluminescence imaging on days 3 and 5 after intrasplenic infusion. (B and C) Quantification of bioluminescence imaging of mice on days 3 and 5 after hepatocyte transplantation. Data are shown as the means ± SEMs (n = 3). *$p < 0.05$.

infused hepatocytes can engraft the recipient liver.[21] Therefore, low cell engraftment needs to be overcome to fully reveal the clinical applications of hepatocyte transplantation. In the present study, we found that ROCK (Rho-associated kinase) inhibitors significantly enhanced *in vivo* hepatocyte engraftment through rationale-based chemical screening. Current studies have suggested that the isolation of hepatocytes causes substantial degradation of cell membrane proteins, including the complement inhibitor CD59, probably due to shear stress-induced endocytosis. ROCK inhibition can protect transplanted hepatocytes by retaining membrane CD59, blocking the formation of the membrane attack complex and significantly enhancing hepatocyte engraftment. Our work reveals a mechanism underlying hepatocyte loss after transplantation and provides immediate strategies to enhance hepatocyte engraftment by inhibiting ROCK.

RESULTS

ROCK inhibition enhances hepatocyte liver engraftment

Massive cell loss occurring soon after hepatocyte infusion represents a huge hurdle for cell therapy of liver diseases. Our initial hypothesis is that liver engraftment of hepatocytes should be improved by enhancing hepatocyte survival or functions. When isolated from naive tissue, epithelial cells can undergo dissociation-induced apoptosis (anoikis). For cultured epithelia, including human pluripotent stem cells, cell dissociation can cause hypercontraction of actomyosin and subsequent apoptosis due to the disruption of cell-cell interactions.[22,23] Previous studies demonstrated that inhibition of ROCK or its downstream nonmuscle myosin II ATPase dramatically improved the survival of dissociated human pluripotent stem cells and other epithelial cells by alleviating the hyperactivation of actomyosin.[22–26] Another study identified a β1-integrin agonist, pyrintegrin, that can enhance the survival of human pluripotent stem cells following enzymatic dissociation by promoting cell extracellular matrix adhesion. The study of our group also indicated that inhibition of actomyosin contraction and YAP activation using a small molecular cocktail, including latrunculin B (an actin polymerization inhibitor); blebbistatin (a nonmuscle myosin II ATPase inhibitor); dasatinib (a Src kinase inhibitor); XAV939 (a tankyrase inhibitor); and LY294002 (a PI3K inhibitor), maintained the functions of hepatocytes.[27] In the present study, we tested the effects of four compounds, ripasudil (ROCK inhibitor), blebbistatin, pyrintegrin, and dasatinib, on the liver engraftment of syngeneic hepatocytes. We first used adeno-associated virus (AAV) expressing luciferase to label hepatocytes of C57 mice (Figure S1). Hepatocytes expressing luciferase were transplanted into syngeneic C57 mice. The compounds were administered soon after cell transplantation. Among the tested compounds, we fortuitously found that the ROCK inhibitor ripasudil dramatically enhanced hepatocyte liver engraftment (Figure 1). The daily time course of flux values of transplanted hepatocytes with ripasudil treatment was analyzed for 7 days (Figure S2). We then tested RKI-1447, another highly specific ROCK inhibitor with a different chemical scaffold from that of ripasudil. RKI-1447 treatment also significantly enhanced hepatocyte liver engraftment (Figure S3). We initially assumed that ROCK inhibition may increase hepatocyte liver engraftment by improving hepatocyte survival. However, neither ripasudil nor RKI-1447 treatment during hepatocyte isolation improved the viability of isolated hepatocytes (Figure S4).

ROCK inhibition blocks complement activation

Given the essential roles of the innate immune system in early hepatocyte loss after infusion,[18] we next analyzed whether ROCK inhibition modulated the function of Kupffer cells, the resident macrophages of the liver. F4/80 immunostaining was used to reveal Kupffer cells on liver sections at 3, 6, and 12 h after mTmG hepatocyte

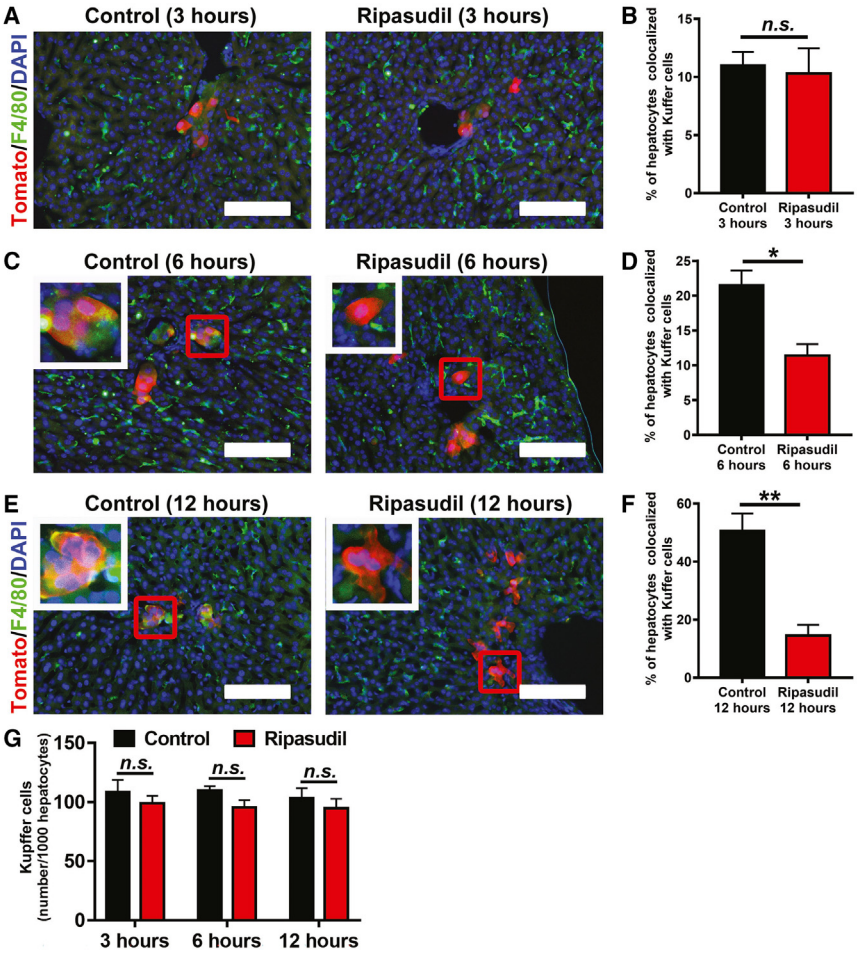

Figure 2. Ripasudil blocked the Kupffer cell activation after hepatocyte transplantation

(A–F) F4/80 immunostaining of liver sections was used to reveal Kupffer cells at 3, 6, and 12 h after transplantation of mTmG hepatocytes. The percentage of hepatocytes colocalized with Kupffer cells was quantified at 3, 6, and 12 h after transplantation of mTmG hepatocytes. The inset in (C) and (E) is a higher-magnification view of the area in the red box of each subpanel. (G) The number of Kupffer cells was quantified and normalized to the hepatocyte number in liver sections. The scale bars represent 100 μM in (A)–(C). Data are expressed as the means ± SEMs of three independent experiments. n.s, no significance. *$p < 0.05$. **$p < 0.01$.

transplantation. At 3 h after cell transplantation, no obvious colocalization was observed between infused tomato-positive hepatocytes and F4/80-positive Kupffer cells (Figures 2A and 2B). However, approximately 21.53% and 50.70% of tomato-positive hepatocytes were colocalized with Kupffer cells at 6 and 12 h after cell transplantation, respectively (Figures 2C–2F). Ripasudil treatment significantly decreased the colocalization between transplanted hepatocytes and Kupffer cells to 11.38% at 6 h and 14.49% at 12 h after transplantation (Figures 2C–2F). In contrast to a previous study,[28] we did not find a significant difference in Kupffer cell number in livers at the studied time points after hepatocyte transplantation (Figure 2G).

As our data showed that ripasudil promoted hepatocyte liver engraftment by inhibiting Kupffer cells, we hypothesized that depletion of macrophages could compromise the effects of ripasudil. Clodronate liposomes are widely used for the suppression of macrophage functions. Clodronate-containing liposomes can be preferentially taken up by macrophages, allowing an effective clodronate concentration threshold to trigger cell apoptosis.[29] Surprisingly, despite the complete clearance of Kupffer cells in livers by clodronate liposome administration (Figure 3A), ripasudil treatment still increased hepatocyte engraftment (Figures 3B and 3C), indicating an indeterministic role of Kupffer cells in ripasudil-enhanced hepatocyte engraftment. These data suggest that ripasudil may function through a mechanism upstream of Kupffer cell phagocytosis.

Previous studies suggested the important role of complement activation in early hepatocyte loss following transplantation.[30] We then analyzed whether ripasudil could modulate the activation of the complement system. Using an *in vitro* complement activation assay in which isolated hepatocytes were incubated with freshly prepared mouse serum, we found that ripasudil treatment dramatically inhibited membrane attack complex formation on hepatocytes, as displayed by C5b-9 staining (Figure 4A). After incubation with serum, 33.53% of hepatocytes were positive for C5b-9 in the control treatment. In contrast, only 7.13% of hepatocytes were positive for C5b-9 under ripasudil treatment (Figures 4A and 4B). Then, we stained live cells with Zombie Red, a fixable fluorescent dye that is nonpermeable, to evaluate the viability of hepatocytes after serum incubation. Consistently, C5b-9 deposition precisely colocalized with Zombie Red cell viability dye staining (Figure 4C), indicating cell membrane disruption of C5b-9-positive hepatocytes. These data suggested that ripasudil treatment protected hepatocytes by preventing the formation of the pore-forming membrane attack complex. The phagocytic clearance of transplanted hepatocytes likely occurred secondarily after this complement attack.

We then tested whether ripasudil could block complement activation *in vivo*. Mice were transplanted with mTmG hepatocytes and treated with ripasudil or vehicle control. Liver tissue was harvested for C5b-9 staining 12 h after transplantation. Ripasudil treatment almost completely blocked C5b-9 deposition on hepatocytes (Figures 5A and 5B). Approximately 49.62% of hepatocytes were positive for C5b-9 at 12 h after transplantation in control mice. In contrast, only 4.38% of mTmG hepatocytes were positive for C5-b9 in ripasudil-treated mice (Figures 5A and 5B). These data further confirmed that ripasudil could protect hepatocytes from host complement attack.

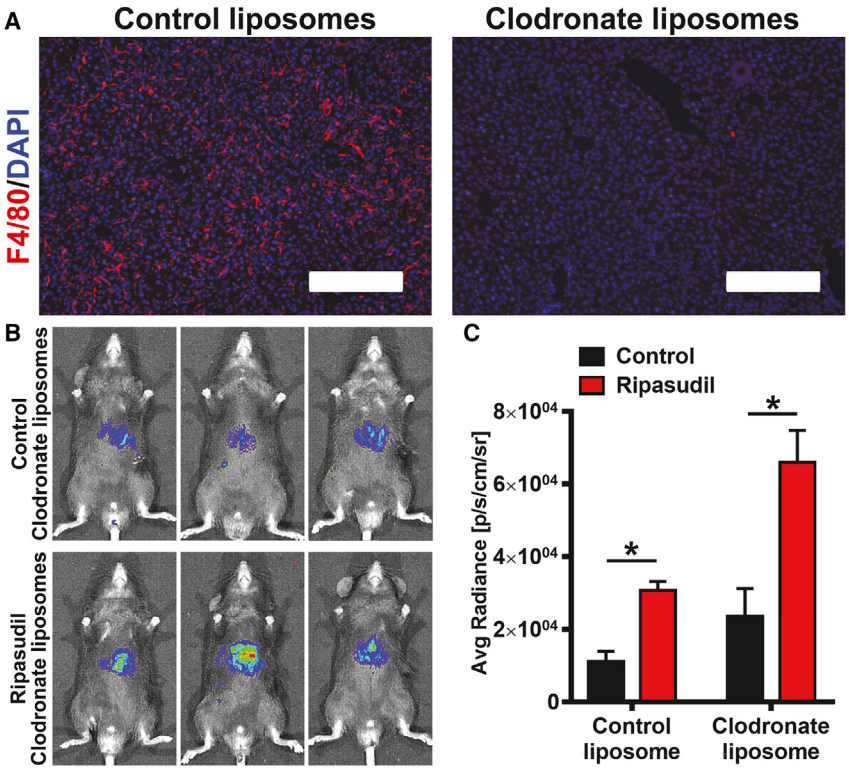

Figure 3. Depletion of Kupffer cells did not abolish the effects of ripasudil on hepatocyte liver engraftment

(A) Clodronate liposomes were used to deplete Kupffer cells in the liver, as revealed by F4/80 immunostaining. (B and C) The engraftment of hepatocytes in livers after depletion of Kupffer cells was analyzed by bioluminescence imaging at 3 days after cell transplantation. The scale bars represent 200 μM in (A). Data are shown as the means ± SEMs (n = 3). *p < 0.05.

Ripasudil stabilized the membrane attack complex inhibitor CD59a on hepatocytes

Next, we focused on the mechanisms by which ripasudil blocks complement activation. Xu et al. reported that the dissociation of human pluripotent stem cells by trypsin induced the endocytosis of cell membrane E-cadherin, which could be blocked by the ROCK inhibitor thiazovivin.[26] Complement activation is tightly regulated by multiple inhibitors that are integral membrane proteins. We therefore hypothesized that ROCK inhibition might block complement activation by maintaining the integrity of cell surface complement inhibitors. We first used pHrodo Red dextran, a pH-sensitive fluorescent dextran, to stain live hepatocytes for imaging of endocytosis. Interestingly, freshly isolated hepatocytes displayed active endocytosis, which could be inhibited by ripasudil treatment (Figure S5A). Consistent with a previous study,[26] ripasudil treatment also maintained membrane E-cadherin on hepatocytes, as revealed by E-cadherin immunostaining (Figure S5B). Western blot assays further confirmed that hepatocyte extraction caused substantial loss of E-cadherin protein, which could be rescued by ripasudil treatment (Figure S5C).

Next, we tried to determine which cell surface complement inhibitors were expressed by hepatocytes. RNA sequencing (RNA-seq) data (GEO: GSE138158) from our previous study showed that hepatocytes expressed high levels of the cell surface membrane attack complex inhibitor CD59a (Figure S6). Other complement inhibitors, including CD46, CD55, CD55b, and CD59b, were expressed at much lower levels (FPKM < 0.5) (Figure S6). We therefore focused on CD59a expression on hepatocytes.

CD59a immunostaining showed very few isolated hepatocytes (approximately 9.73%) with predominant CD59a membrane localization (Figures 6A and 6B). However, 58.29% of hepatocytes displayed strong CD59a membrane localization under ripasudil treatment. Western blot assays showed rapid loss of CD59a protein on isolated hepatocytes, which could be blocked by ripasudil treatment (Figures 6C and 6D). Puromycin, but not actinomycin D, blocked the effects of ripasudil in maintaining E-cadherin and CD59a protein levels. These data suggest that ROCK inhibition maintains hepatocyte membrane protein homeostasis and that this is dependent on protein neosynthesis (Figure S7). Real-time PCR assays revealed that ripasudil treatment did not have a significant impact on CD59a mRNA expression (Figure 6E), suggesting a posttranscriptional mechanism underlying the downregulation of CD59a protein in isolated hepatocytes. Notably, the expression of CD59a was not uniform among hepatocytes. After incubation with mouse serum, the staining of CD59a and C5b-9 demonstrated a mutually exclusive pattern. Only hepatocytes with weak cell membrane CD59a expression exhibited C5b-9 deposition (Figures 6F and 6G). These data were consistent with the function of CD59a as a membrane attack complex inhibitor and supported the notion that ripasudil enhanced hepatocyte liver engraftment by stabilizing cell surface CD59a.

To confirm that ripasudil functions through CD59a, the expression of CD59a on hepatocytes was knocked down by short hairpin RNA (shRNA) transduced using an AAV vector. Western blot and real-time PCR assays confirmed the dramatic downregulation of CD59a after shRNA transduction, especially by CD59a shRNA2 (Figures 7A–7C). Then, hepatocytes transduced with CD59a shRNA2 were isolated for the *in vitro* complement activation assay. After incubation with mouse serum, CD59a knockdown caused a significant increase in C5b-9 deposition on hepatocytes, which could no longer be blocked by ripasudil treatment (Figures 7D and 7E). Consistently, ripasudil treatment did not enhance the liver engraftment of hepatocytes with diminished expression of CD59a (Figures 7F and

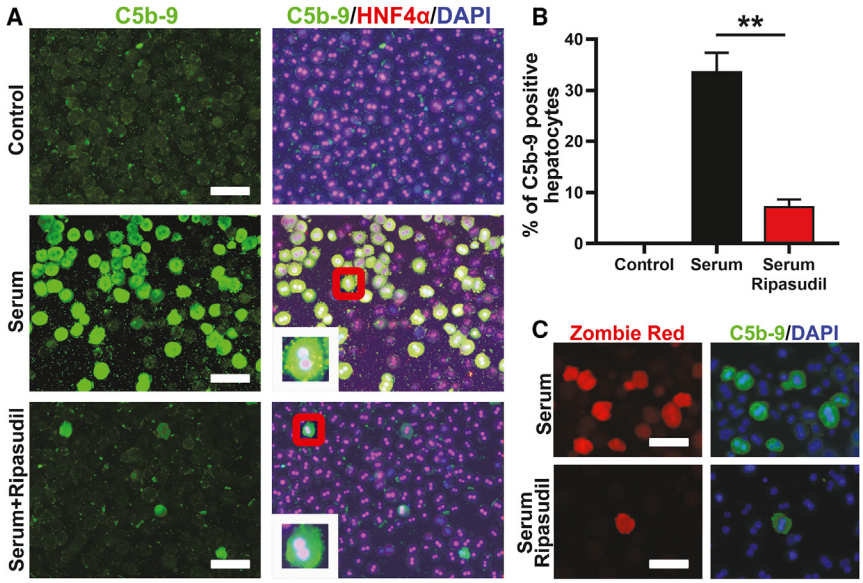

Figure 4. Ripasudil blocked membrane attack complex formation on hepatocytes after incubation with mouse serum *in vitro*

(A) C5b-9 and HNF4a immunostaining of hepatocytes incubated with fresh mouse serum was used to reveal the formation of the membrane attack complex. The inset in (A) is a higher-magnification view of the area in the red box of each subpanel. (B) C5b-9-positive hepatocytes were quantified under different treatments. (C) The viability of hepatocytes after serum incubation was analyzed by Zombie Red fixable dye staining. The scale bars represent 50 μM in (A) and (C). Data are shown as the means ± SEMs of three independent experiments. **p < 0.01.

7G) but significantly enhanced the liver engraftment of hepatocytes transduced with scramble shRNA (Figure S8). These data confirmed that CD59a was a major complement inhibitor on hepatocytes, and CD59a knockdown impaired hepatocyte engraftment, which could not be rescued by ripasudil.

Next, we used pAAV-TBG-CD59a-WPRE to overexpress CD59a in hepatocytes. Immunostaining and western blot assays confirmed the up-regulation of CD59a in transduced hepatocytes (Figures S9A and S9B). Then, the hepatocytes from mTmG mice transduced with pAAV-TBG-Cd59a-WPRE (red hepatocytes) and mTmG mice transduced with pAAV-TBG-Cre-WPRE (green hepatocytes) were pooled together at a 1:1 ratio (Figures S9C and S9D) and transplanted into wild-type C57 mice. Overexpression of CD59a significantly enhanced hepatocyte engraftment, and ripasudil treatment did not enhance the liver engraftment of hepatocytes with CD59a overexpression (Figures S9E and S9F).

Ripasudil accelerates liver repopulation of fumarylacetoacetate hydrolase (Fah)-deficient mice and synergizes with irradiation to further improve hepatocyte engraftment

Next, we analyzed whether ripasudil could accelerate liver repopulation of $Fah^{-/-}$ mice after hepatocyte transplantation.[31] Fah deficiency causes tyrosinemia and fatal liver damage. $Fah^{-/-}$ mice can be maintained by supplying them with 2-(2-nitro-4-trifluoromethylbenzoyl)-1,3-cyclo hexanedione (NTBC), an inhibitor of 4-hydroxyphenylpyruvate dioxygenase. Upon NTBC withdrawal, low-dose hepatocytes (105 cells per mouse, equivalent to approximately 0.05% of all hepatocytes in a host liver) from wild-type C57 mice were transplanted into $Fah^{-/-}$ mice intrasplenically, and the mice were treated with ripasudil for the first 3 days. The mice were analyzed at 2, 3, and 4 weeks. There were significantly more Fah-positive hepatocyte colonies in ripasudil-treated $Fah^{-/-}$ mice at the analyzed time points after cell infusion (Figure 8A). The transplanted cells integrated into the host liver with expression of the bile canaliculus marker Dpp4 (Figure 8A). Fah-positive hepatocytes repopulated 0.11% and 0.41%, 0.21% and 0.65%, and 0.52% and 3.96% of the liver parenchyma at 2, 3, and 4 weeks in the control and ripasudil-treated recipients, respectively (Figure 8B). Consistently, liver function of $Fah^{-/-}$ mice in the ripasudil-treated group was significantly improved at 4 weeks as revealed by serum analysis of alanine aminotransferase (ALT) and aspartate aminotransferase (AST) (Figures 8C and 8D). All $Fah^{-/-}$ mice survived after hepatocyte transplantation. However, the experiments were terminated at 4 weeks after cell infusion due to the poor condition of the mice in the control group. To rule out the possibility that ripasudil treatment improved liver function in $Fah^{-/-}$ mice, serum ALT and AST levels of $Fah^{-/-}$ mock transplant ripasudil-treated mice and $Fah^{-/-}$ mock transplant vehicle-treated mice in the absence of NTBC for 4 weeks were analyzed (Figure S10). Ripasudil treatment had no impact on serum ALT or AST levels.

Liver irradiation has been shown to improve hepatocyte engraftment and proliferation.[32] Preparative hepatic irradiation before hepatocyte transplantation was applied in human subjects with classical phenylketonuria.[33] Irradiation-enhanced engraftment is likely mediated by temporary disruption of hepatic sinusoidal endothelial cells in the short term and endows transplanted cells with a proliferative advantage in the long term. Given the different mechanisms of irradiation and ROCK inhibition in promoting hepatocyte engraftment, we next tested whether ROCK inhibition could synergize with hepatic irradiation in hepatocyte transplantation. Consistent with a previous study,[32] hepatic irradiation alone dramatically enhanced hepatocyte engraftment in the host liver (Figure S11). Importantly, ROCK inhibition can synergize with irradiation to further improve hepatocyte engraftment (Figure S11).

DISCUSSION

Hepatocyte transplantation offers a promising alternative to liver transplantation for end-stage liver diseases. However, poor hepatocyte engraftment is a fundamental issue that must be overcome to reveal its full therapeutic potential. Previous study suggested that only approximately 2%–6% of infused hepatocytes can engraft the

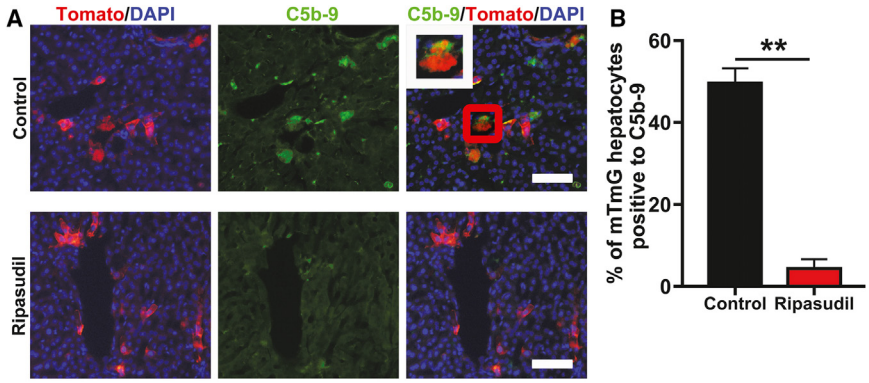

Figure 5. Ripasudil blocked C5b-9 deposition on transplanted hepatocytes *in vivo*

(A) C5b-9 immunostaining of liver sections 12 h after mTmG hepatocyte transplantation under control or ripasudil treatment. The inset in (A) is a higher magnification view of the area in the red box. (B) C5b-9positive mTmG hepatocytes were quantified under ripasudil or control treatment. The scale bars represent 100 μM in (A). Data are shown as the means ± SEMs of three independent experiments. **p < 0.01.

recipient liver.[21] The liver weight of adult 8-to 10-week-old C57BL6 male mice is approximately 1.5 g, and they bear approximately 2×10^8 hepatocytes.[34] After infusing 1×10^6 hepatocytes, transplanted cells can engraft 0.1%–0.25% of the host liver under ripasudil treatment in our experiments (Figures 5 and S9), which translates to approximately 20%–50% cell engraftment after transplantation.

Previous studies have provided compelling evidence that the IBMIR is responsible for the significant loss of transplanted hepatocytes.[35–37] The IBMIR is characterized by activation of the coagulation and complement cascade systems, by leukocytic infiltration, and by phagocytosis. However, how the coagulation pathway activates the complement system is not well defined. Our present work revealed a mechanism by which the degradation of the cell surface complement inhibitor CD59, probably due to hyperendocytosis-induced membrane protein internalization, causes complement activation and donor hepatocyte death. The shear stress experienced by hepatocytes during liver perfusion and cell dissociation may trigger this hyperendocytosis in isolated hepatocytes. A previous study indicated that fluid shear stress can induce profound internalization of cell membrane proteins through endocytosis.[38,39] This study also indicated that administration of the ROCK inhibitor ripasudil is a feasible approach to inhibiting endocytosis and maintaining cell surface protein integrity. As ripasudil has already been licensed for treating ocular hypertension and open-angle glaucoma, it has potential for rapid translation as a therapeutic to boost hepatocyte transplantation.

However, this study did have some limitations. For example, how ROCK inhibition blocks the endocytosis of isolated hepatocytes remains unclear. A previous study showed that ROCK2 promotes CD59 internalization through clathrin-independent endocytosis by regulating myosin II contractility.[40] Whether ripasudil functions through a similar mechanism needs further investigation. In addition, whether the isolation procedure causes global hepatocyte membrane protein endocytosis and degradation remains to be determined. The present study demonstrated that ROCK inhibition-enhanced hepatocyte engraftment relies on membrane CD59a. However, whether inhibition of membrane attack complex (MAC) by CD59a is the only mechanism in promoting hepatocyte liver engraftment remains to be determined.

Many attempts have been made to improve cell engraftment after liver infusion. Administration of antiinflammatory agents, e.g., the tumor necrosis factor α (TNF-α) inhibitors etanercept and thalidomide and the innate immune modulator α-1 antitrypsin, and blockage of the coagulant cascade using coagulation inhibitors improved the engraftment of transplanted hepatocytes.[36,37,41–45] In addition, the survival of transplanted hepatocytes was considerably increased *in vivo* by treatment of graft recipients with hepatic sinusoidal vasodilators[46,47] or gadolinium chloride to deplete Kupffer cells.[28] Additionally, preconditioning of the liver through partial hepatectomy,[48,49] portal embolization,[50] and irradiation[33,51] could enhance cell transplantation by providing a selective proliferative advantage to the transplanted cells. It would be interesting to test whether there are synergistic effects when these approaches are combined with ROCK inhibition.

IBMIR-induced cell damage is not unique to hepatocyte transplantation. Transplantation of islets of Langerhans and mesenchymal stem cells has been associated with significant cell loss soon after administration,[52,53] leading to compromised efficacy. Whether cell isolation-/dissociation-induced cell surface loss of complement inhibitors was also involved in the triggering of the IBMIR for these applications needs to be further investigated.

MATERIALS AND METHODS

Mice

Normal male C57BL/6 mice, aged 8 to 10 weeks, were obtained from Shanghai SLAC Laboratory Animals (specific-pathogen-free grade). *Fah*$^{-/-}$ mice of the C57BL/6 background were obtained from Shanghai MODEL organisms and were maintained by adding 7.5 mg/L NTBC to the drinking water. mTmG mice were ordered from the Jackson Laboratory. All animals were housed in a temperature- and light-controlled (12-h light/dark cycle) specific pathogen-free (SPF) animal facility. All animal procedures were performed in accordance with institutional guidelines.

In vivo AAV infection

Replication-incompetent AAV2/8-CAG-EGFP-T2A-lucifrase (Obio Technology, Shanghai, China) was used to transduce hepatocytes of C57BL/6 mice via tail vein injection at 2×10^{11} genome copies of virus per mouse. To knock down *CD59a* (NM_007652.5) in

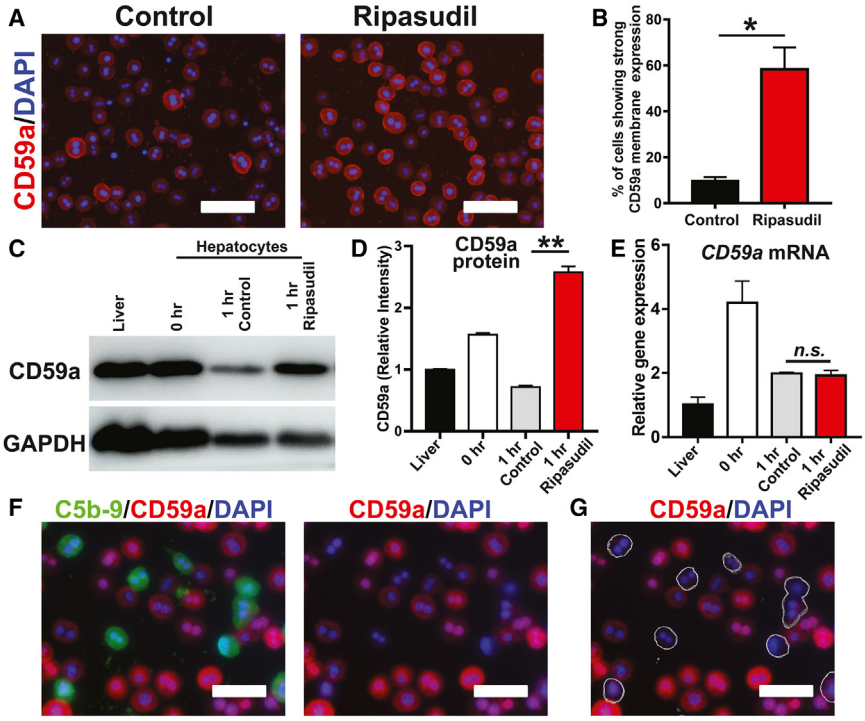

Figure 6. Ripasudil blocked membrane attack complex formation by stabilizing membrane CD59a

(A) The expression of CD59a in freshly isolated hepatocytes was analyzed by immunostaining after an hour of treatment with ripasudil or vehicle control. (B) The membrane expression of CD59a was quantified. (C and D) The expression of CD59a in liver tissue and freshly isolated hepatocytes was analyzed by western blotting. (E) CD59a mRNA expression was analyzed by real-time PCR. (F and G) Costaining of C5b-9 and CD59a was performed on hepatocytes incubated with mouse serum. C5b-9-positive hepatocytes are delineated with a thin outline in (G). The scale bars represent 50 μM in (A), (F), and (G). Data are shown as the means ± SEMs of three independent experiments. *$p < 0.05$, **$p < 0.01$.

hepatocytes, shRNA sequences targeting mouse *CD59a* were cloned into the pAAV-CMV-Luc2-WPRE-U6-spgRNA vector (Obio Technology) to generate pAAV-CMV-Luc2-WPRE-U6-*CD59a* shRNA. The hairpin sequences used in this study are described in Table S1. To overexpress *CD59a* (NM_007652.5), *CD59a* cDNA was synthesized and cloned into pAAV-TBG-MCS-3xFLAG-WPRE to generate pAAV-TBG-CD59a-WPRE. Replication-incompetent AAV2/8-CMV-Luc2-WPRE-U6-CD59a shRNA, AAV2/8- CMV-Luc2-WPRE-U6-scramble shRNA, pAAV-TBG-CD59a-WPRE, and pAAV-TBG-NLS-Cre-3xFLAG-WPRE packaged and purified by Obio Technology were administered to 8-week-old C57BL/6 mice through tail vein injection at 2×10^{11} genome copies of virus per mouse. Mouse hepatocytes were harvested for analysis 14 days after AAV transduction.

Hepatocyte isolation and transplantation

Mouse primary hepatocytes were isolated by two-step collagenase perfusion via the portal vein. Primary liver cell suspensions were centrifuged two times at 50 g for 5 min. The hepatocyte pellet was suspended in serum-free DMEM/F12. Cell viability was measured by the trypan blue exclusion assay. Hepatocytes were transplanted into 8-week-old wild-type C57 mice through splenic injection. Each mouse received 200 μL cell suspension containing 1×10^6 viable hepatocytes.

For transplantation in irradiation preconditioned mice, normal male C57BL/6 mice, aged 8 to 10 weeks, were subjected to a single dose of 20 Gy abdominal gamma ray irradiation from a cobalt-60 source. Irradiation was limited to the upper abdomen of the mouse by customized 50-mm lead shielding of other parts of the body. Hepatocyte transplantation was performed 24 h after irradiation.

In vivo chemical screening

Wild-type mice infused with hepatocytes transduced with AAV2/8-CAG-EGFP-T2A-lucifrase were used for *in vivo* screening. The compounds screened were ripasudil (ROCK inhibitor, 17.3 mg/kg body weight); dasatinib (Src kinase inhibitor, 25 mg/kg body weight); blebbistatin (nonmuscle myosin II ATPase inhibitor, 2.5 mg/kg body weight); and pyrintegrin (β1-integrin agonist, 10 mg/kg body weight). All chemicals were first dissolved in DMSO and diluted in 30% 2-hydroxypropyl-β-cyclodextrin at a ratio of 1:20 to generate the working solution. All mice received compounds at the indicated dosage soon after cell transplantation by intraperitoneal injection (working solution or vehicle control at 10 mL/kg body weight). The mice were analyzed by *in vivo* bioluminescence imaging after luciferin (PerkinElmer) injection (150 μg luciferin/kg body weight) at the time points indicated. In subsequent experiments to analyze the function of ripasudil on hepatocyte engraftment, ripasudil was administered on days 0, 1, and 2 after transplantation. All chemicals were obtained from MedChemExpress except where mentioned.

In vitro assay for complement activation

Mouse blood was collected intracardially. Briefly, mice were euthanized in a carbon dioxide chamber. A 25G needle connected with a 1-mL syringe was inserted into the chest while maintaining a constant slight negative aspiration pressure. Once all the blood was withdrawn, the needle was removed from the syringe, and the blood was collected into a 1.5-mL Eppendorf tube without anticoagulant. The blood was allowed to clot for 30 min at 4°C before centrifugation at 1,300 RCF for 15 min. Serum was collected, pooled, and immediately used for *in vitro* complement activation assays.

For *in vitro* complement activation assays, isolated hepatocytes were cultured in Matrigel-coated 12-well plates at 1×10^5 cells/well using 700 μL DMEM/F12 medium supplemented with N2 and B27, as previously reported.[27] Hepatocytes were cultured for an hour with 4 μM ripasudil or vehicle control. Then, freshly collected mouse serum

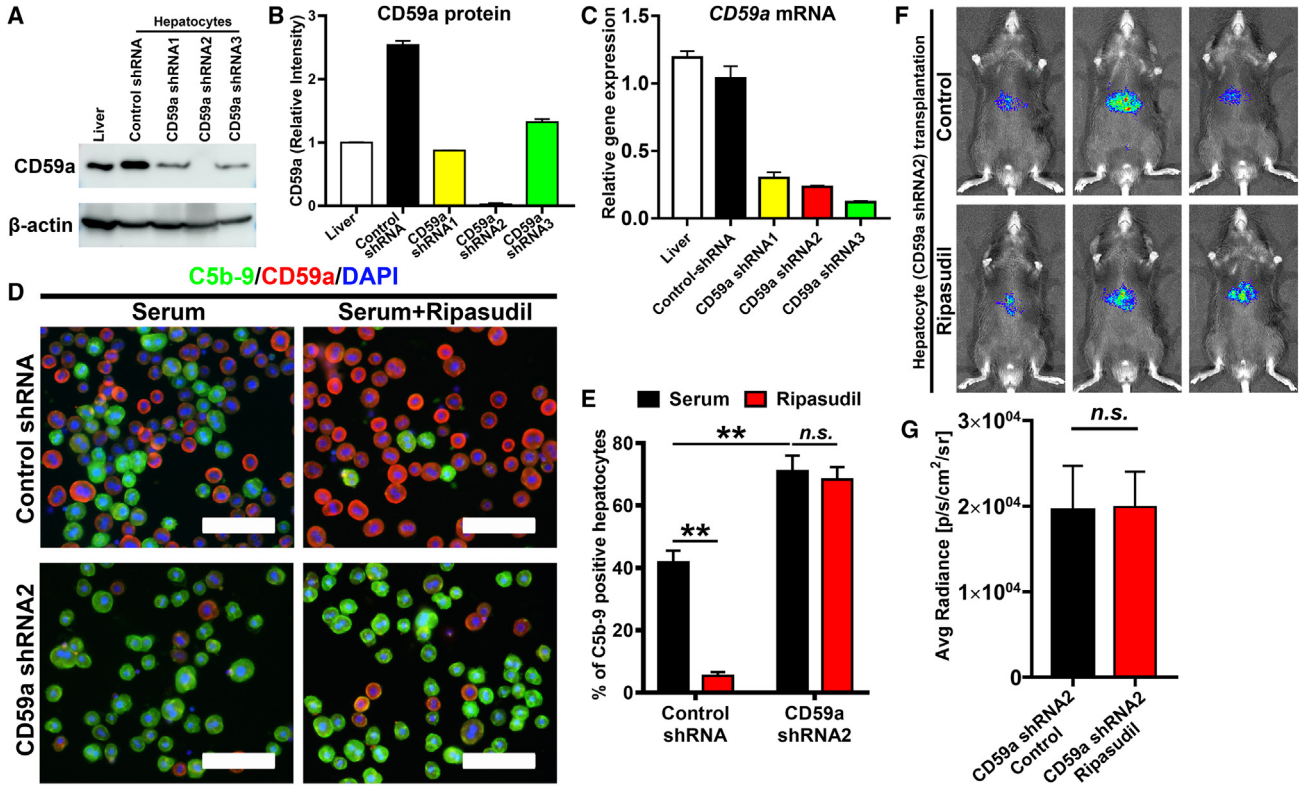

Figure 7. Knockdown of CD59a abolished ripasudil-enhanced hepatocyte liver engraftment

(A) Protein bands of western blot analysis of CD59a expression by hepatocytes after transduction with AAV expressing CD59a shRNA. (B) Gray value analysis of (A). (C) Real-time PCR analysis of CD59a expression by hepatocytes after transduction with AAV expressing CD59a shRNA. (D) Costaining of C5b-9 and CD59a was performed on hepatocytes incubated with fresh serum after knock down of CD59a. (E) Quantitative analysis of C5b-9 positive hepatocytes in (D). (F) The liver engraftment of hepatocytes expressing CD59a shRNA2 was analyzed by bioluminescence imaging 3 days after cell transplantation. (G) Quantitative analysis of (F). The scale bars represent 100 μM in (D). Data are shown as the means ± SEMs of three independent experiments. *$p < 0.05$, **$p < 0.01$.

(300 μL per well) was added to each well. After incubation for another hour, hepatocytes were fixed in 4% paraformaldehyde for analysis of the membrane attack complex by C5b-9 staining. Zombie Red fixable dye staining (BioLegend) was performed according to the manufacturer's instructions.

All tissue culture products were obtained from Invitrogen except where mentioned.

Immunocytochemistry and histology analysis

For immunocytochemistry analysis, cells were fixed in 4% paraformaldehyde for 5 min at 4°C, washed three times with PBST (PBS containing 0.1% Triton X-100), and incubated in blocking buffer consisting of PBST with 5% normal donkey serum (Jackson ImmunoResearch Laboratories) for 30 min at room temperature. The cells were then incubated with primary antibody overnight at 4°C in blocking buffer. Next, the cells were washed with PBST and incubated with Alexa Fluor-conjugated secondary antibodies (Invitrogen, 1,000×) in PBST for 1 h at room temperature. Nuclei were visualized by DAPI staining (Sigma-Aldrich). Images were captured using a Nikon Eclipse 50i microscope. Counting of fluorescent cells in immunocytochemistry images was performed using ImageJ software as previously reported.[54] The images were converted to binary images. The staining threshold was implemented manually. Ten random 100× visual fields were selected to obtain the mean values for each staining.

For the histology assays, liver tissues were fixed in 4% paraformaldehyde overnight at 4°C and embedded in optimal cutting temperature (OCT) compound. Liver cryostat sections (10 μm) were floated in PBST, washed three times, and incubated in blocking buffer for 30 min at room temperature. The sections were then incubated with primary antibody overnight at 4°C in blocking buffer. After washing with PBST, the sections were incubated with Alexa Fluor-conjugated secondary antibodies (Invitrogen, 1,000×) in PBST for 1 h at room temperature. Nuclei were visualized by DAPI staining (Sigma-Aldrich). Images were captured using a Nikon Eclipse Ti2-U microscope. Quantification of Fah-positive or mTmG hepatocytes in the liver was performed in cryostat sections of left liver lobes. Ten random 100× visual fields from different sections were selected to obtain the mean value for every mouse (at least three mice at each time points) by using ImageJ software.

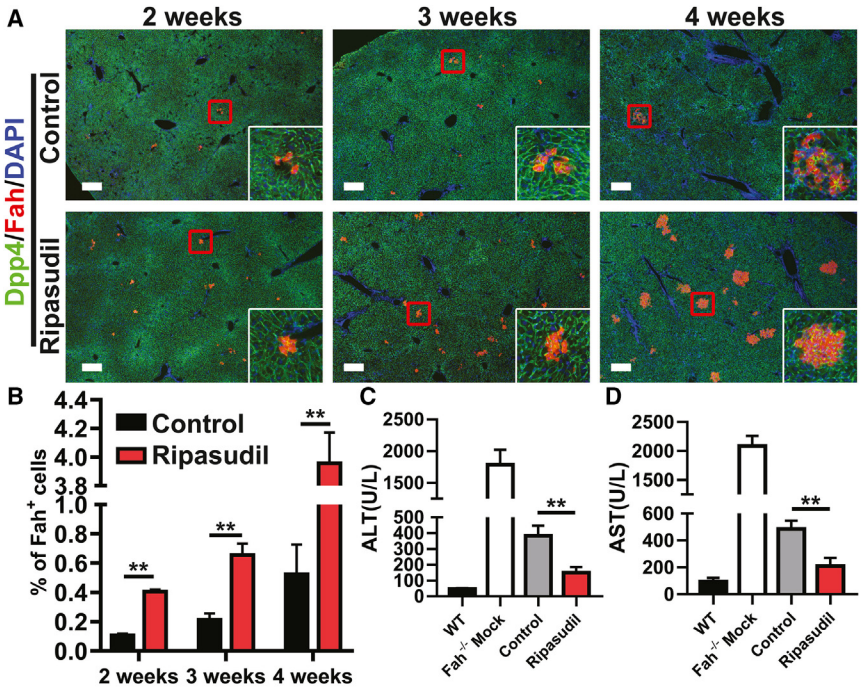

Figure 8. Ripasudil accelerates liver repopulation of *Fah*$^{-/-}$ mice

(A) Dpp4 and Fah costaining of *Fah*$^{-/-}$ mouse liver sections 2, 3, and 4 weeks after wild-type hepatocyte transplantation under treatment with ripasudil or vehicle control. The inset in (A) is a higher-magnification view of the area in the red box of each image. (B) The percentage of liver engraftment at 2, 3, and 4 weeks was quantified. (C and D) Serum analysis of alanine aminotransferase (ALT) and aspartate aminotransferase (AST) in *Fah*$^{-/-}$ mice 4 weeks after hepatocyte transplantation under treatment with ripasudil or vehicle control. The scale bars represent 250 μM in (A). Data are shown as the means ± SEMs. $^{**}p < 0.01$.

The antibodies used are shown in Table S2.

RNA extraction and qRT-PCR analysis

RNA was extracted using RNAiso Plus reagents (TaKaRa). Reverse transcription was performed with 1 μg RNA using PrimeScript RT Master Mix (TaKaRa). The primers used are shown in Table S3. qRT-PCR was carried out using PowerUp SYBR Green mixture (Thermo Fisher Scientific). The expression of CD59a was normalized to that of GAPDH in all samples.

TRANSPLANTATION OF *FAH*$^{-/-}$ MICE

Twenty-four *Fah*$^{-/-}$ mice were divided into two groups. One group received 1×10^5 viable hepatocytes (n = 12) and was intraperitoneally administered 17.3 mg/kg/day ripasudil soon after cell transplantation once a day for 3 days. The second group received 1×10^5 viable hepatocytes (n = 12) and was administered vehicle control intraperitoneally soon after cell transplantation once a day for 3 days. NTBC was removed from the drinking water soon after cell transplantation. The animals were analyzed at 2 (n = 3 for each group), 3 (n = 3 for each group), and 4 weeks (n = 6 for each group). Six *Fah*$^{-/-}$ mice receiving 200 μL PBS through splenic injection were used as mock transplantation controls and were administered vehicle control intraperitoneally once a day for 3 days.

Quantification and statistical analysis

Statistical analysis was performed using GraphPad Prism 7 software unless otherwise noted. Statistical significance (p values) was calculated by unpaired two-tailed Student's t test. Statistical significance was denoted as follows: $^{*}p < 0.05$; $^{**}p < 0.01$; n.s., not significant.

DATA AVAILABILITY

The data that support the findings of this study are available from the corresponding author upon reasonable request.

SUPPLEMENTAL INFORMATION

Supplemental information can be found online at https://doi.org/10.1016/j.ymthe.2023.02.018.

ACKNOWLEDGMENTS

This study was supported by the National Key R&D Program of China (grant no. 2018YFA0107200),National Natural Science Foundation of China (grant nos. 32170851, 92168118, and 81571094), and Program of Shanghai Academic Research Leader (grant no. 17XD1404800).

AUTHOR CONTRIBUTIONS

H.M., Chao Wang (second author), and S.L. performed hepatocyte isolation, chemical screening, *in vivo* hepatocyte transplantation, and histological analysis. X.Y., Y.Y., Z.L., and C.J. performed hepatocyte culture and immunofluorescence analysis. J. Zhang and J. Zhu performed genotyping analysis of *Fah*$^{-/-}$ mice and real-time PCR analysis. Each author analyzed their own data. W.L., P.S., and Chao Wang (tenth author) conceived and supervised the project. W.L. wrote the manuscript with input from co-authors.

DECLARATION OF INTERESTS

The authors declare no competing interests.

REFERENCES

1. Asrani, S.K., Devarbhavi, H., Eaton, J., and Kamath, P.S. (2019). Burden of liver diseases in the world. J. Hepatol. *70*, 151–171. https://doi.org/10.1016/j.jhep.2018.09.014.

2. Weber, A., Mahieu-Caputo, D., Hadchouel, M., and Franco, D. (2006). Hepatocyte transplantation: studies in preclinical models. J. Inherit. Metab. Dis. *29*, 436–441. https://doi.org/10.1007/s10545-006-0253-8.

3. Dwyer, B.J., Macmillan, M.T., Brennan, P.N., and Forbes, S.J. (2021). Cell therapy for advanced liver diseases: repair or rebuild. J. Hepatol. *74*, 185–199. https://doi.org/10.1016/j.jhep.2020.09.014.

4. Viswanathan, P., and Gupta, S. (2012). New directions for cell-based therapies in acute liver failure. J. Hepatol. *57*, 913–915. https://doi.org/10.1016/j.jhep.2012.06.009.

5. Forbes, S.J., Gupta, S., and Dhawan, A. (2015). Cell therapy for liver disease: from liver transplantation to cell factory. J. Hepatol. *62*, S157–S169. https://doi.org/10.1016/j.jhep.2015.02.040.

6. Mito, M., Kusano, M., and Kawaura, Y. (1992). Hepatocyte transplantation in man. Transpl. Proc. *24*, 3052–3053.

7. Hansel, M.C., Gramignoli, R., Skvorak, K.J., Dorko, K., Marongiu, F., Blake, W., Davila, J., and Strom, S.C. (2014). The history and use of human hepatocytes for the treatment of liver diseases: the first 100 patients. Curr. Protoc. Toxicol. *62*, 11–23. https://doi.org/10.1002/0471140856.tx1412s62.

8. Nguyen, M.P., Jain, V., Iansante, V., Mitry, R.R., Filippi, C., and Dhawan, A. (2020). Clinical application of hepatocyte transplantation: current status, applicability, limitations, and future outlook. Expert Rev. Gastroenterol. Hepatol. *14*, 185–196. https://doi.org/10.1080/17474124.2020.1733975.

9. Dhawan, A., Puppi, J., Hughes, R.D., and Mitry, R.R. (2010). Human hepatocyte transplantation: current experience and future challenges. Nat. Rev. Gastroenterol. Hepatol. *7*, 288–298. https://doi.org/10.1038/nrgastro.2010.44.

10. Stéphenne, X., Najimi, M., Sibille, C., Nassogne, M.C., Smets, F., and Sokal, E.M. (2006). Sustained engraftment and tissue enzyme activity after liver cell transplantation for argininosuccinate lyase deficiency. Gastroenterology *130*, 1317–1323. https://doi.org/10.1053/j.gastro.2006.01.008.

11. Luce, E., Messina, A., Duclos-Vallée, J.C., and Dubart-Kupperschmitt, A. (2021). Advanced techniques and awaited clinical applications for human pluripotent stem cell differentiation into hepatocytes. Hepatology *74*, 1101–1116. https://doi.org/10.1002/hep.31705.

12. Levy, G., Bomze, D., Heinz, S., Ramachandran, S.D., Noerenberg, A., Cohen, M., Shibolet, O., Sklan, E., Braspenning, J., and Nahmias, Y. (2015). Long-term culture and expansion of primary human hepatocytes. Nat. Biotechnol. *33*, 1264–1271. https://doi.org/10.1038/nbt.3377.

13. Zhang, K., Zhang, L., Liu, W., Ma, X., Cen, J., Sun, Z., Wang, C., Feng, S., Zhang, Z., Yue, L., et al. (2018). *In vitro* expansion of primary human hepatocytes with efficient liver repopulation capacity. Cell stem cell *23*, 806–819.e804. https://doi.org/10.1016/j.stem.2018.10.018.

14. Mun, S.J., Ryu, J.S., Lee, M.O., Son, Y.S., Oh, S.J., Cho, H.S., Son, M.Y., Kim, D.S., Kim, S.J., Yoo, H.J., et al. (2019). Generation of expandable human pluripotent stem cell-derived hepatocyte-like liver organoids. J. Hepatol. *71*, 970–985. https://doi.org/10.1016/j.jhep.2019.06.030.

15. Hu, H., Gehart, H., Artegiani, B., LÖpez-Iglesias, C., Dekkers, F., Basak, O., van Es, J., Chuva de Sousa Lopes, S.M., Begthel, H., Korving, J., et al. (2018). Long-term expansion of functional mouse and human hepatocytes as 3D organoids. Cell *175*, 1591–1606.e19. https://doi.org/10.1016/j.cell.2018.11.013.

16. Peng, W.C., Logan, C.Y., Fish, M., Anbarchian, T., Aguisanda, F., Álvarez-Varela, A., Wu, P., Jin, Y., Zhu, J., Li, B., et al. (2018). Inflammatory cytokine TNFα promotes the long-term expansion of primary hepatocytes in 3D culture. Cell *175*, 1607–1619.e15. https://doi.org/10.1016/j.cell.2018.11.012.

17. Unzu, C., Planet, E., Brandenberg, N., Fusil, F., Cassano, M., Perez-Vargas, J., Friedli, M., Cosset, F.-L., Lutolf, M.P., Wildhaber, B.E., and Trono, D. (2019). Pharmacological induction of a progenitor state for the efficient expansion of primary human hepatocytes. Hepatology *69*, 2214–2231. https://doi.org/10.1002/hep.30425.

18. Iansante, V., Mitry, R.R., Filippi, C., Fitzpatrick, E., and Dhawan, A. (2018). Human hepatocyte transplantation for liver disease: current status and future perspectives. Pediatr. Res. *83*, 232–240. https://doi.org/10.1038/pr.2017.284.

19. Gupta, S., Rajvanshi, P., Sokhi, R., Slehria, S., Yam, A., Kerr, A., and Novikoff, P.M. (1999). Entry and integration of transplanted hepatocytes in rat liver plates occur by disruption of hepatic sinusoidal endothelium. Hepatology *29*, 509–519. https://doi.org/10.1002/hep.510290213.

20. Krohn, N., Kapoor, S., Enami, Y., Follenzi, A., Bandi, S., Joseph, B., and Gupta, S. (2009). Hepatocyte transplantation-induced liver inflammation is driven by cytokines-chemokines associated with neutrophils and Kupffer cells. Gastroenterology *136*, 1806–1817. https://doi.org/10.1053/j.gastro.2009.01.063.

21. Wang, L.J., Chen, Y.M., George, D., Smets, F., Sokal, E.M., Bremer, E.G., and Soriano, H.E. (2002). Engraftment assessment in human and mouse liver tissue after sex-mismatched liver cell transplantation by real-time quantitative PCR for Y chromosome sequences. Liver Transplant. *8*, 822–828. https://doi.org/10.1053/jlts.2002.34891.

22. Ohgushi, M., Matsumura, M., Eiraku, M., Murakami, K., Aramaki, T., Nishiyama, A., Muguruma, K., Nakano, T., Suga, H., Ueno, M., et al. (2010). Molecular pathway and cell state responsible for dissociation-induced apoptosis in human pluripotent stem cells. Cell stem cell *7*, 225–239. https://doi.org/10.1016/j.stem.2010.06.018.

23. Chen, G., Hou, Z., Gulbranson, D.R., and Thomson, J.A. (2010). Actin-myosin contractility is responsible for the reduced viability of dissociated human embryonic stem cells. Cell stem cell *7*, 240–248. https://doi.org/10.1016/j.stem.2010.06.017.

24. Lv, L., Han, Q., Chu, Y., Zhang, M., Sun, L., Wei, W., Jin, C., and Li, W. (2015). Self-renewal of hepatoblasts under chemically defined conditions by iterative growth factor and chemical screening. Hepatology *61*, 337–347. https://doi.org/10.1002/hep.27421.

25. Watanabe, K., Ueno, M., Kamiya, D., Nishiyama, A., Matsumura, M., Wataya, T., Takahashi, J.B., Nishikawa, S.i., Nishikawa, S., Muguruma, K., and Sasai, Y. (2007). A ROCK inhibitor permits survival of dissociated human embryonic stem cells. Nat. Biotechnol. *25*, 681–686. https://doi.org/10.1038/nbt1310.

26. Xu, Y., Zhu, X., Hahm, H.S., Wei, W., Hao, E., Hayek, A., and Ding, S. (2010). Revealing a core signaling regulatory mechanism for pluripotent stem cell survival and self-renewal by small molecules. Proc. Natl. Acad. Sci. USA *107*, 8129–8134. https://doi.org/10.1073/pnas.1002024107.

27. Sun, P., Zhang, G., Su, X., Jin, C., Yu, B., Yu, X., Lv, Z., Ma, H., Zhang, M., Wei, W., and Li, W. (2019). Maintenance of primary hepatocyte functions in vitro by inhibiting mechanical tension-induced YAP activation. Cell Rep. *29*, 3212–3222.e4. https://doi.org/10.1016/j.celrep.2019.10.128.

28. Joseph, B., Malhi, H., Bhargava, K.K., Palestro, C.J., McCuskey, R.S., and Gupta, S. (2002). Kupffer cells participate in early clearance of syngeneic hepatocytes transplanted in the rat liver. Gastroenterology *123*, 1677–1685. https://doi.org/10.1053/gast.2002.36592.

29. van Rooijen, N., and van Kesteren-Hendrikx, E. (2002). Clodronate liposomes: perspectives in research and therapeutics. J. Liposome Res. *12*, 81–94. https://doi.org/10.1081/lpr-120004780.

30. Kocken, J.M., Bouwman, E., Scheringa, M., Borel Rinkes, I.H., Bruijn, J.A., Sinaasappel, M., and Terpstra, O.T. (1997). Acute death after intraportal hepatocyte transplantation in an allogeneic rat strain combination: a possible role for complement activation. Transpl. Proc. *29*, 2067–2068. https://doi.org/10.1016/s0041-1345(97)00235-2.

31. Overturf, K., al-Dhalimy, M., Ou, C.N., Finegold, M., and Grompe, M. (1997). Serial transplantation reveals the stem-cell-like regenerative potential of adult mouse hepatocytes. Am. J. Pathol. *151*, 1273–1280.

32. Yamanouchi, K., Zhou, H., Roy-Chowdhury, N., Macaluso, F., Liu, L., Yamamoto, T., Yannam, G.R., Enke, C., Solberg, T.D., Adelson, A.B., et al. (2009). Hepatic irradiation augments engraftment of donor cells following hepatocyte transplantation. Hepatology *49*, 258–267. https://doi.org/10.1002/hep.22573.

33. Soltys, K.A., Setoyama, K., Tafaleng, E.N., Soto Gutiérrez, A., Fong, J., Fukumitsu, K., Nishikawa, T., Nagaya, M., Sada, R., Haberman, K., et al. (2017). Host conditioning and rejection monitoring in hepatocyte transplantation in humans. J. Hepatol. *66*, 987–1000. https://doi.org/10.1016/j.jhep.2016.12.017.

34. Sohlenius-Sternbeck, A.K. (2006). Determination of the hepatocellularity number for human, dog, rabbit, rat and mouse livers from protein concentration measurements. Toxicol. Vitro. *20*, 1582–1586. https://doi.org/10.1016/j.tiv.2006.06.003.

35. Sullivan, B.P., Kopec, A.K., Joshi, N., Cline, H., Brown, J.A., Bishop, S.C., Kassel, K.M., Rockwell, C., Mackman, N., and Luyendyk, J.P. (2013). Hepatocyte tissue factor activates the coagulation cascade in mice. Blood *121*, 1868–1874. https://doi.org/10.1182/blood-2012-09-455436.

36. Stéphenne, X., Vosters, O., Najimi, M., Beuneu, C., Dung, K.N., Wijns, W., Goldman, M., and Sokal, E.M. (2007). Tissue factor-dependent procoagulant activity of isolated human hepatocytes: relevance to liver cell transplantation. Liver Transplant. *13*, 599–606. https://doi.org/10.1002/lt.21128.

37. Gustafson, E.K., Elgue, G., Hughes, R.D., Mitry, R.R., Sanchez, J., Haglund, U., Meurling, S., Dhawan, A., Korsgren, O., and Nilsson, B. (2011). The instant blood-mediated inflammatory reaction characterized in hepatocyte transplantation. Transplantation *91*, 632–638. https://doi.org/10.1097/TP.0b013e31820ae459.

38. He, Z., Zhang, W., Mao, S., Li, N., Li, H., and Lin, J.M. (2018). Shear stress-enhanced internalization of cell membrane proteins indicated by a hairpin-type DNA probe. Anal. Chem. *90*, 5540–5545. https://doi.org/10.1021/acs.analchem.8b00755.

39. Raghavan, V., Rbaibi, Y., Pastor-Soler, N.M., Carattino, M.D., and Weisz, O.A. (2014). Shear stress-dependent regulation of apical endocytosis in renal proximal tubule cells mediated by primary cilia. Proc. Natl. Acad. Sci. USA *111*, 8506–8511. https://doi.org/10.1073/pnas.1402195111.

40. Wayt, J., Cartagena-Rivera, A., Dutta, D., Donaldson, J.G., and Waterman, C.M. (2021). Myosin II isoforms promote internalization of spatially distinct clathrin-independent endocytosis cargoes through modulation of cortical tension downstream of ROCK2. Mol. Biol. Cell *32*, 226–236. https://doi.org/10.1091/mbc.E20-07-0480.

41. Lee, C.A., Dhawan, A., Smith, R.A., Mitry, R.R., and Fitzpatrick, E. (2016). Instant blood-mediated inflammatory reaction in hepatocyte transplantation: current status and future perspectives. Cell Transpl. *25*, 1227–1236. https://doi.org/10.3727/096368916x691286.

42. Viswanathan, P., Kapoor, S., Kumaran, V., Joseph, B., and Gupta, S. (2014). Etanercept blocks inflammatory responses orchestrated by TNF-α to promote transplanted cell engraftment and proliferation in rat liver. Hepatology *60*, 1378–1388. https://doi.org/10.1002/hep.27232.

43. Viswanathan, P., Gupta, P., Kapoor, S., and Gupta, S. (2016). Thalidomide promotes transplanted cell engraftment in the rat liver by modulating inflammation and endothelial integrity. J. Hepatol. *65*, 1171–1178. https://doi.org/10.1016/j.jhep.2016.07.008.

44. Jaber, F.L., Sharma, Y., Mui, B.G., Kapoor, S., and Gupta, S. (2021). Tumor necrosis factor directs allograft-related innate responses and its neutralization improves hepatocyte engraftment in rats. Am. J. Pathol. *191*, 79–89. https://doi.org/10.1016/j.ajpath.2020.09.014.

45. Lee, C., Dhawan, A., Iansante, V., Filippi, C., Mitry, R., Tang, J., Walker, S., Fernandez DaCosta, R., Sinha, S., Hughes, R.D., et al. (2019). Improving engraftment of hepatocyte transplantation using alpha-1 antitrypsin as an immune modulator. J. Mol. Med. *97*, 563–577. https://doi.org/10.1007/s00109-019-01747-3.

46. Slehria, S., Rajvanshi, P., Ito, Y., Sokhi, R.P., Bhargava, K.K., Palestro, C.J., McCuskey, R.S., and Gupta, S. (2002). Hepatic sinusoidal vasodilators improve transplanted cell engraftment and ameliorate microcirculatory perturbations in the liver. Hepatology *35*, 1320–1328. https://doi.org/10.1053/jhep.2002.33201.

47. Bahde, R., Kapoor, S., Bandi, S., Bhargava, K.K., Palestro, C.J., and Gupta, S. (2013). Directly acting drugs prostacyclin or nitroglycerine and endothelin receptor blocker bosentan improve cell engraftment in rodent liver. Hepatology *57*, 320–330. https://doi.org/10.1002/hep.26005.

48. Jorns, C., Nowak, G., Nemeth, A., Zemack, H., Mörk, L.M., Johansson, H., Gramignoli, R., Watanabe, M., Karadagi, A., Alheim, M., et al. (2016). De novo donor-specific HLA antibody formation in two patients with crigler-najjar syndrome type I following human hepatocyte transplantation with partial hepatectomy preconditioning. Am. J. Transpl. *16*, 1021–1030. https://doi.org/10.1111/ajt.13487.

49. Gupta, S., Johnstone, R., Darby, H., Selden, C., Price, Y., and Hodgson, H.J. (1987). Transplanted isolated hepatocytes: effect of partial hepatectomy on proliferation of long-term syngeneic implants in rat spleen. Pathology *19*, 28–30. https://doi.org/10.3109/00313028709065131.

50. Dagher, I., Boudechiche, L., Branger, J., Coulomb-Lhermine, A., Parouchev, A., Sentilhes, L., Lin, T., Groyer-Picard, M.T., Vons, C., Hadchouel, M., et al. (2006). Efficient hepatocyte engraftment in a nonhuman primate model after partial portal vein embolization. Transplantation *82*, 1067–1073. https://doi.org/10.1097/01.tp.0000236103.99456.8f.

51. Guha, C., Sharma, A., Gupta, S., Alfieri, A., Gorla, G.R., Gagandeep, S., Sokhi, R., Roy-Chowdhury, N., Tanaka, K.E., Vikram, B., and Roy-Chowdhury, J. (1999). Amelioration of radiation-induced liver damage in partially hepatectomized rats by hepatocyte transplantation. Cancer Res. *59*, 5871–5874.

52. Nilsson, B., Ekdahl, K.N., and Korsgren, O. (2011). Control of instant blood-mediated inflammatory reaction to improve islets of Langerhans engraftment. Curr. Opin. Organ Transpl. *16*, 620–626. https://doi.org/10.1097/MOT.0b013e32834c2393.

53. Moll, G., Alm, J.J., Davies, L.C., von Bahr, L., Heldring, N., Stenbeck-Funke, L., Hamad, O.A., Hinsch, R., Ignatowicz, L., Locke, M., et al. (2014). Do cryopreserved mesenchymal stromal cells display impaired immunomodulatory and therapeutic properties? Stem Cells *32*, 2430–2442. https://doi.org/10.1002/stem.1729.

54. Handala, L., Fiore, T., Rouillé, Y., and Helle, F. (2019). QuantIF: an ImageJ macro to automatically determine the percentage of infected cells after immunofluorescence. Viruses *11*. https://doi.org/10.3390/v11020165.

YMTHE, Volume *31*

Supplemental Information

ROCK inhibition enhanced hepatocyte liver engraftment by retaining membrane CD59 and attenuating complement activation

Haoxin Ma, Chao Wang, Shulong Liang, Xinlu Yu, Yuan Yuan, Zhuanman Lv, Jiqianzhu Zhang, Caixia Jin, Jiangbo Zhu, Chao Wang, Pingxin Sun, and Wenlin Li

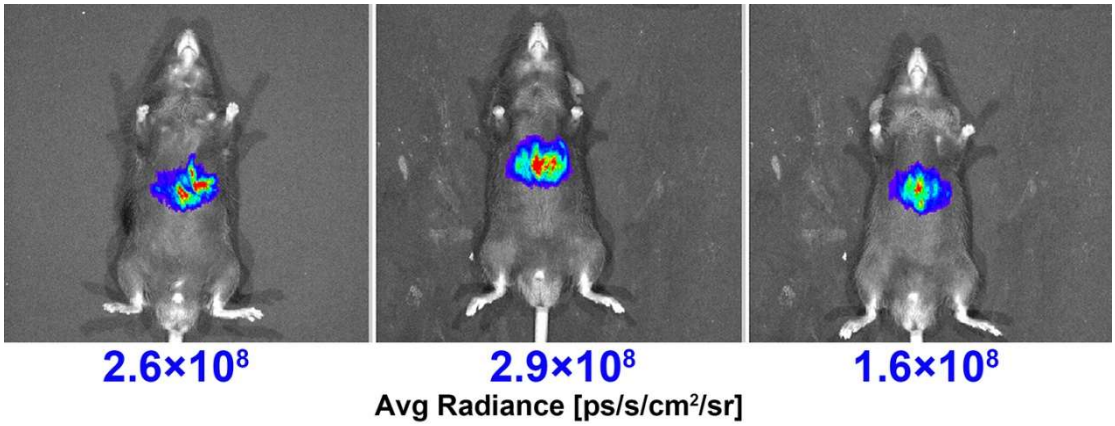

Figure S1. Representative bioluminescence images of mice transduced with replication-incompetent AAV2/8-CAG-EGFP-T2A-lucifrase.

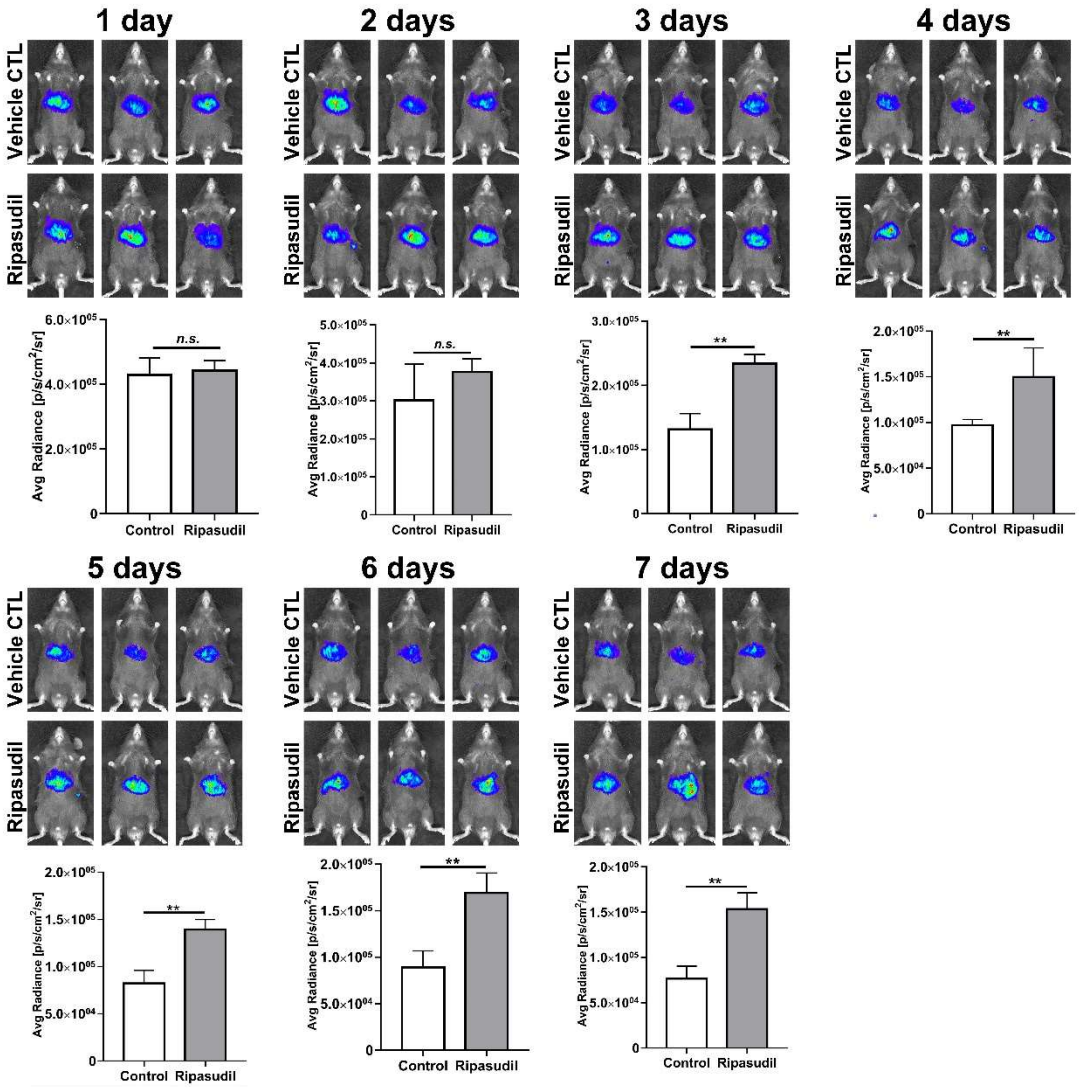

Figure S2. The daily time course of flux values of transplanted hepatocytes with ripasudil treatment for 7 days. Data are shown as the means ± SEMs (n=3). n.s, no significance. ** P<0.01.

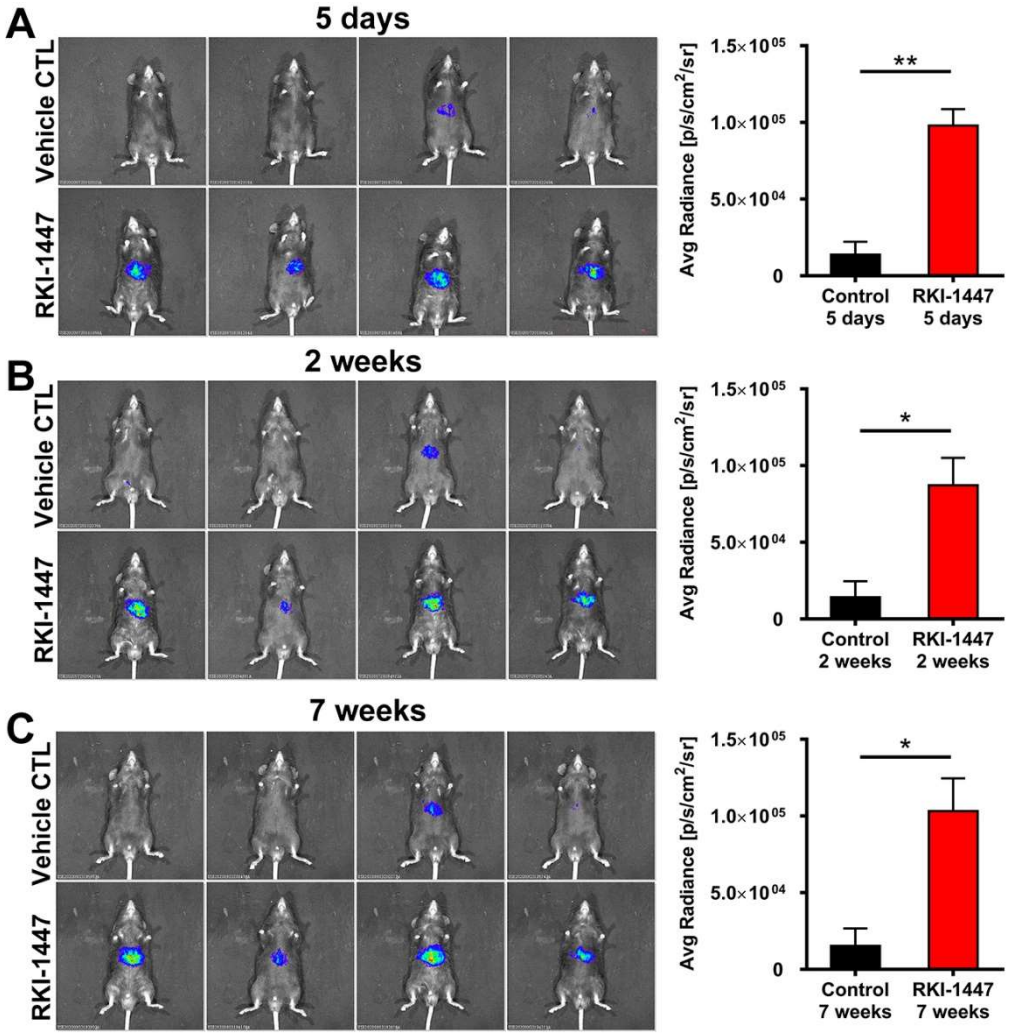

Figure S3. RKI-1447, another ROCK inhibitor with a different chemical scaffold from that of ripasudil, enhances hepatocyte liver engraftment. RKI-1447 (ROCK inhibitor, 80 mg/kg) was administered once intraperitoneally soon after cell transplantation. The mice were analyzed at 5 days, 2 weeks, and 7 weeks after transplantation. Data are shown as the means ± SEMs (n=4). *p < 0.05. ** P<0.01.

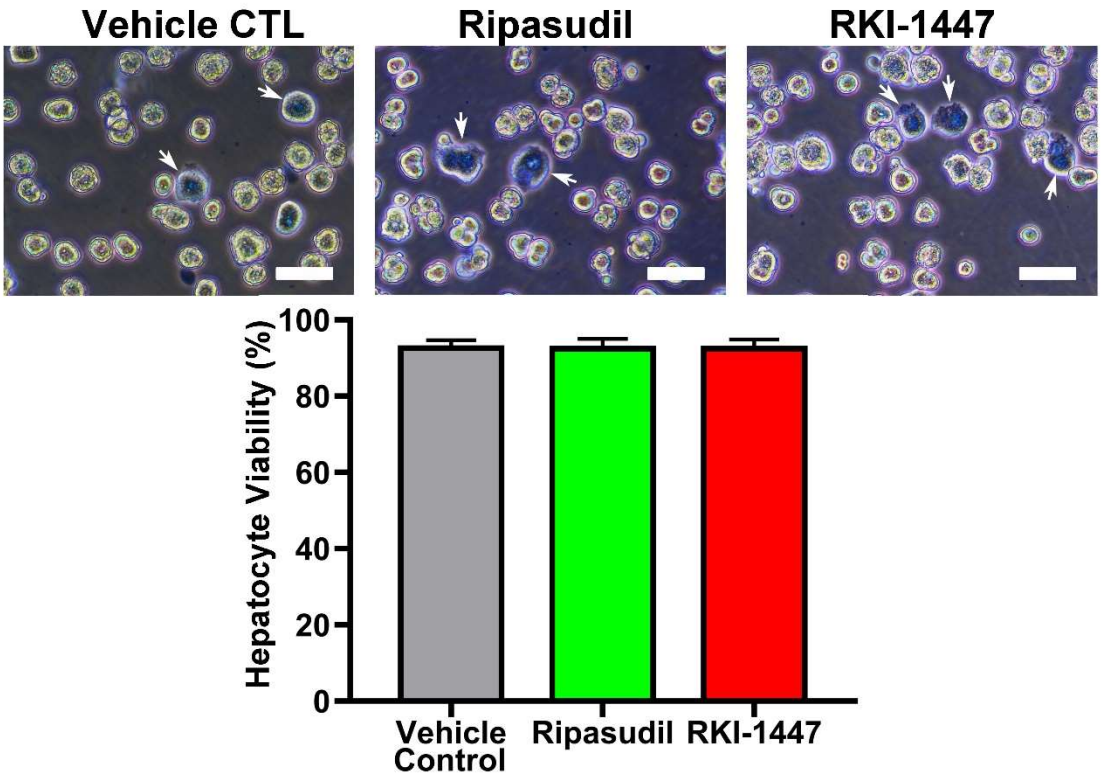

Figure S4. The viability of hepatocytes isolated with perfusion and digestion buffer supplemented with 4 μM ripasudil or RKI-1447. Arrow indicated the cells stained with trypan blue. The scale bars represent 50 μM. Data are expressed as the means ± SEMs of four independent hepatocyte isolation experiments.

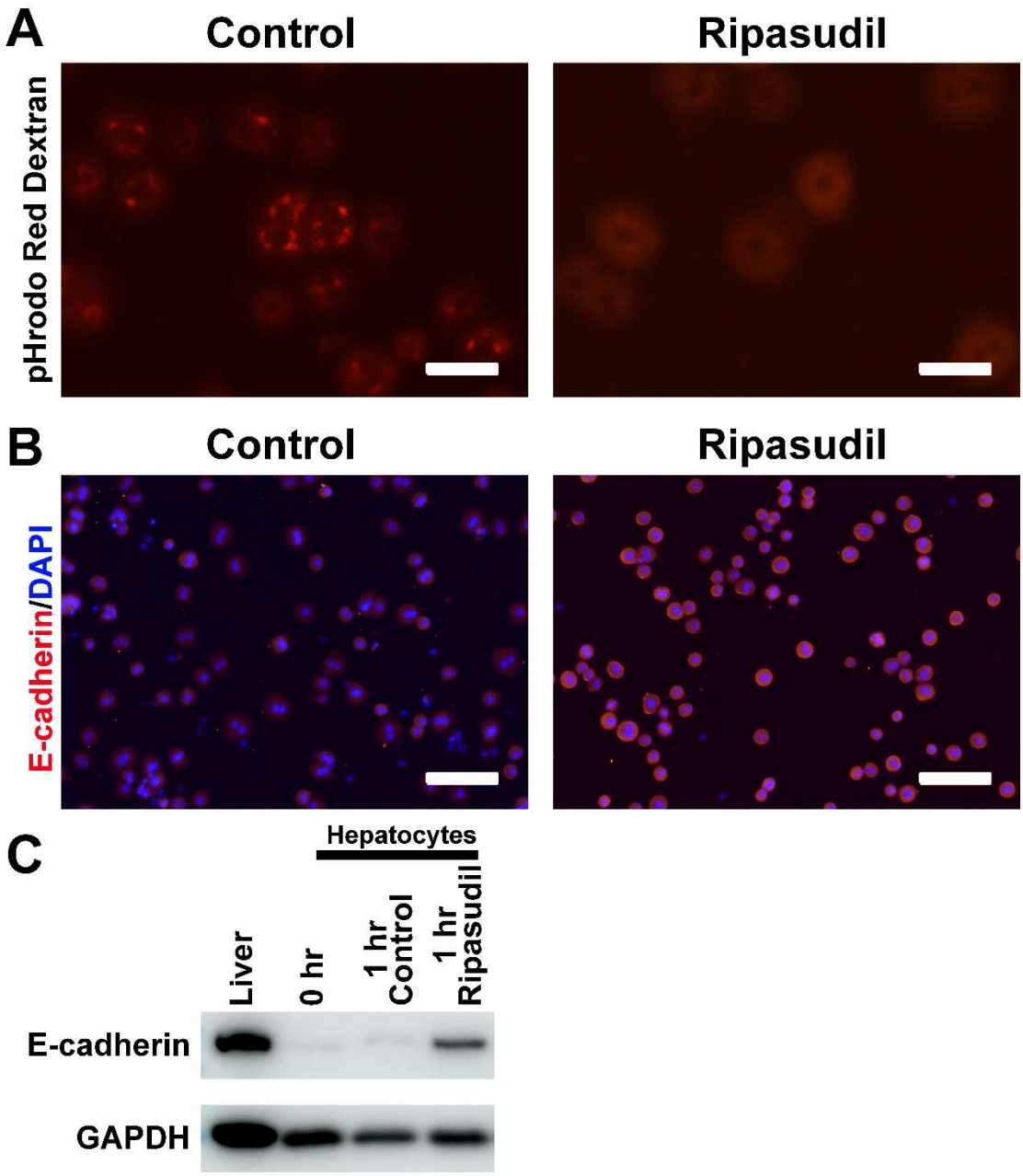

Figure S5. Ripasudil inhibited hepatocyte endocytosis and retained cell membrane E-cadherin. (A) Endocytosis of isolated hepatocytes was demonstrated by pHrodo Red dextran staining. (B) The expression of E-cadherin in isolated hepatocytes was analyzed by immunostaining after treatment with ripasudil or vehicle control. (C) The expression of E-cadherin in the liver and isolated hepatocytes was analyzed by western blotting. The scale bars represent 50 μM in Panel A and 100 μM in Panel B.

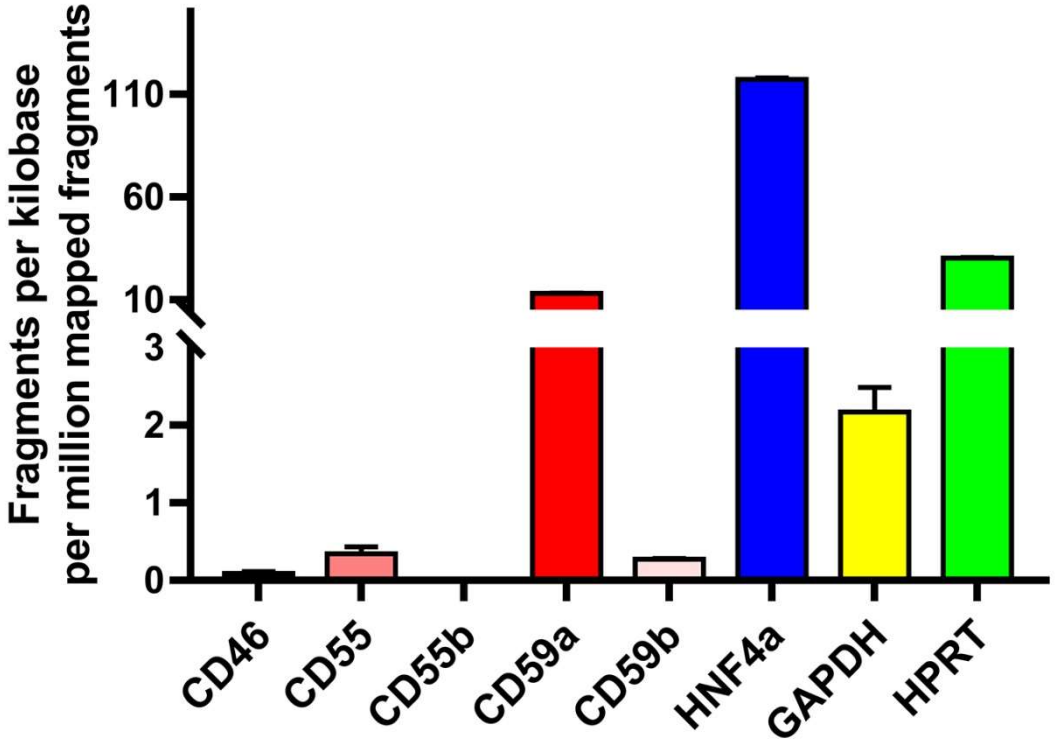

Figure S6. The RNA-seq data (GSE138158) showed that freshly isolated hepatocytes expressed the complement inhibitor CD59a. GSE138158 contains 2 biological repeats of RNA-seq data for freshly isolated hepatocytes.

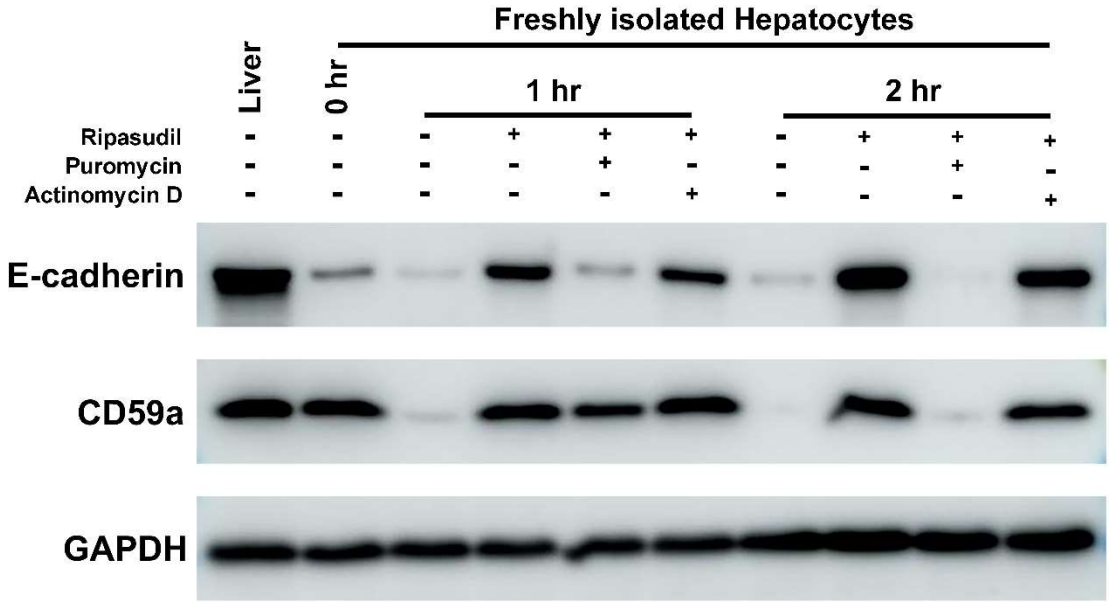

Figure S7. Ripasudil maintains hepatocyte membrane protein homeostasis dependent on protein neosynthesis. The expression of E-cadherin and CD59a in isolated hepatocytes was analyzed by western blotting after treatment with ripasudil, puromycin and actinomycin D.

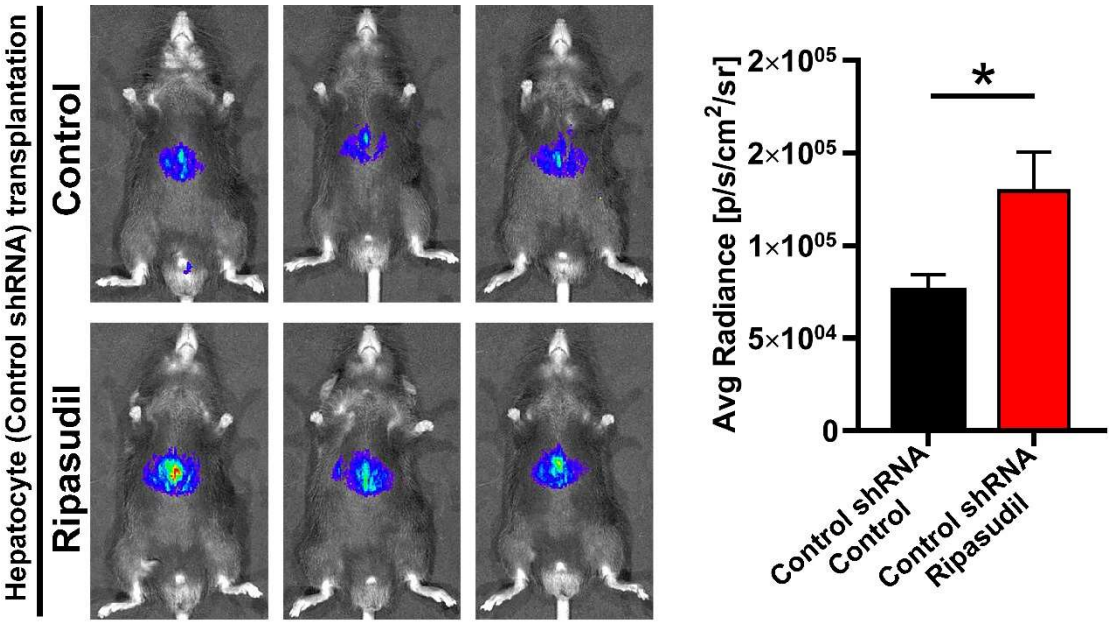

Figure S8. The liver engraftment of hepatocytes expressing control shRNA was analyzed by bioluminescence imaging 3 days after cell transplantation. Data are shown as the means ± SEMs of three independent experiments. *p < 0.05.

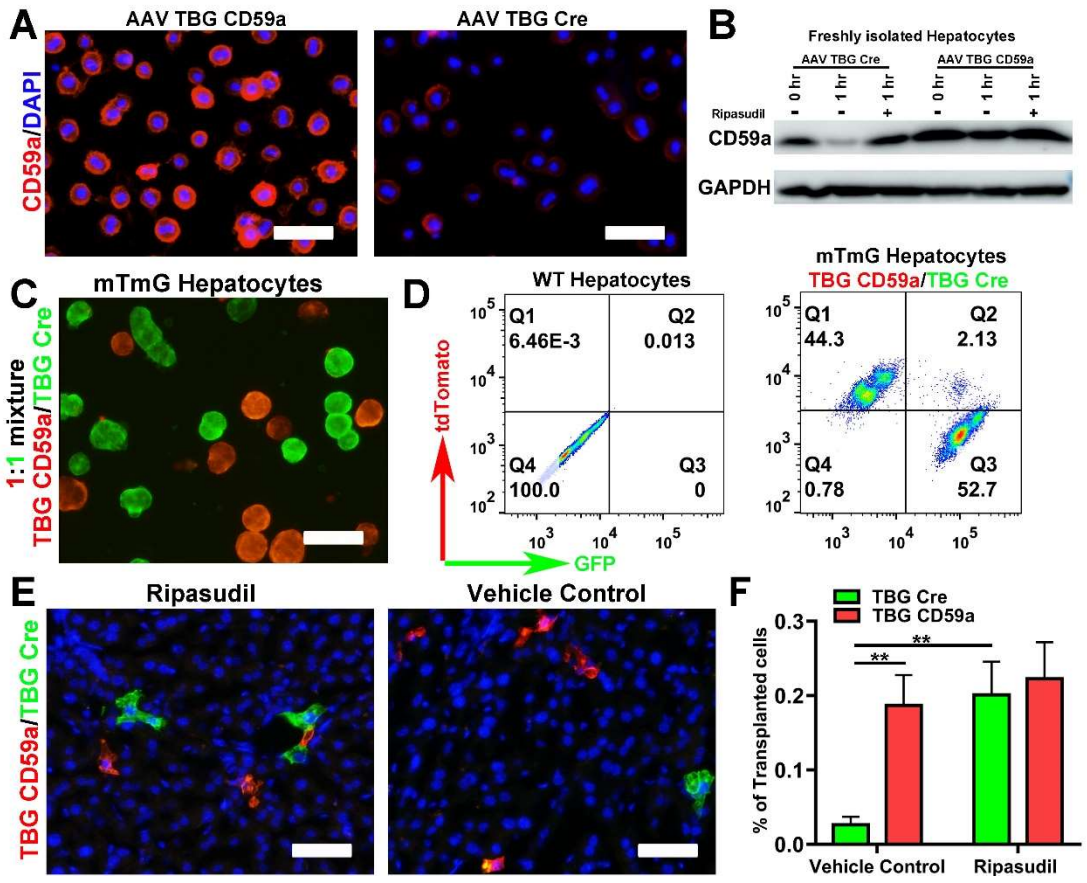

Figure S9. Overexpression of CD59a enhanced hepatocyte liver engraftment. (A) The expression of CD59a in isolated hepatocytes transduced with pAAV-TBG-Cd59a-WPRE or pAAV-TBG-Cre-WPRE was analyzed by immunostaining. (B) CD59a expression by hepatocytes transduced with pAAV-TBG-Cd59a-WPRE or pAAV-TBG-Cre-WPRE was analyzed by western blot. (C and D) Fluorescence images and flow cytometry analysis of 1:1 pooled mTmG hepatocytes transduced with pAAV-TBG-Cd59a-WPRE (red hepatocytes) and pAAV-TBG-Cre-WPRE (green hepatocytes). (E) Fluorescence images of liver sections transplanted with pooled mTmG hepatocytes transduced with pAAV-TBG-Cd59a-WPRE (red hepatocytes) and pAAV-TBG-Cre-WPRE (green hepatocytes). The mice were analyzed at 7 days after transplantation. (F) Quantitative analysis of Panel E. The scale bars represent 50 μM. Data are shown as the means ± SEMs of three

independent experiments. **p < 0.01.

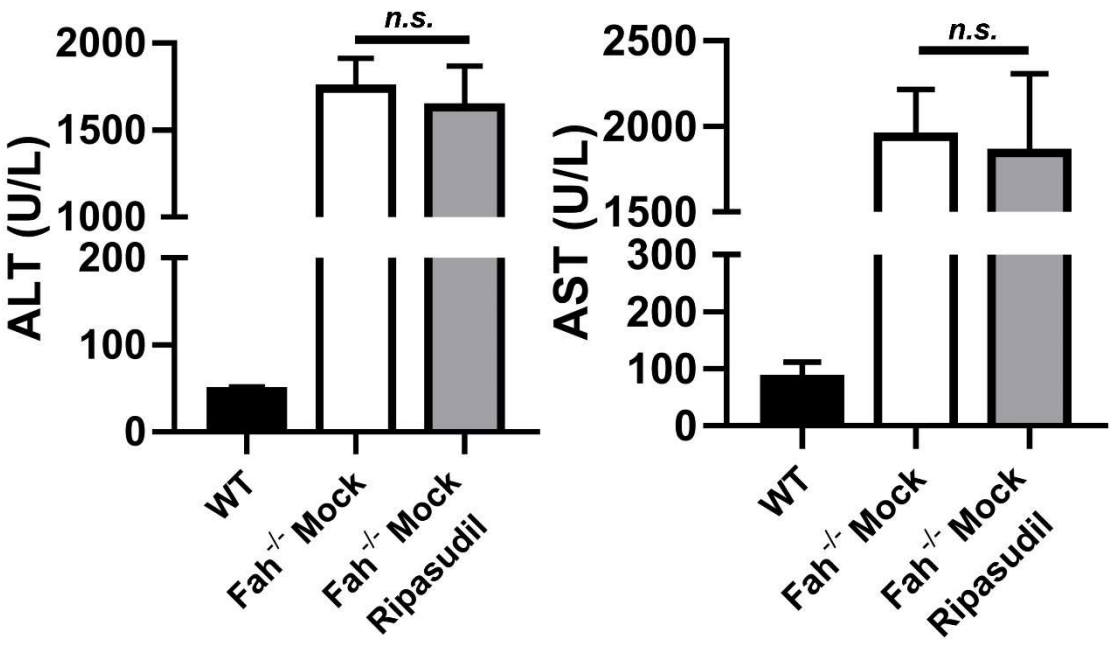

Figure S10. Ripasudil treatment has no impact on liver function in *Fah*$^{-/-}$ mice. Serum analysis of alanine aminotransferase (ALT) and aspartate aminotransferase (AST) in *Fah*$^{-/-}$ mice at 4 weeks after mock transplantation under treatment with ripasudil or vehicle control.

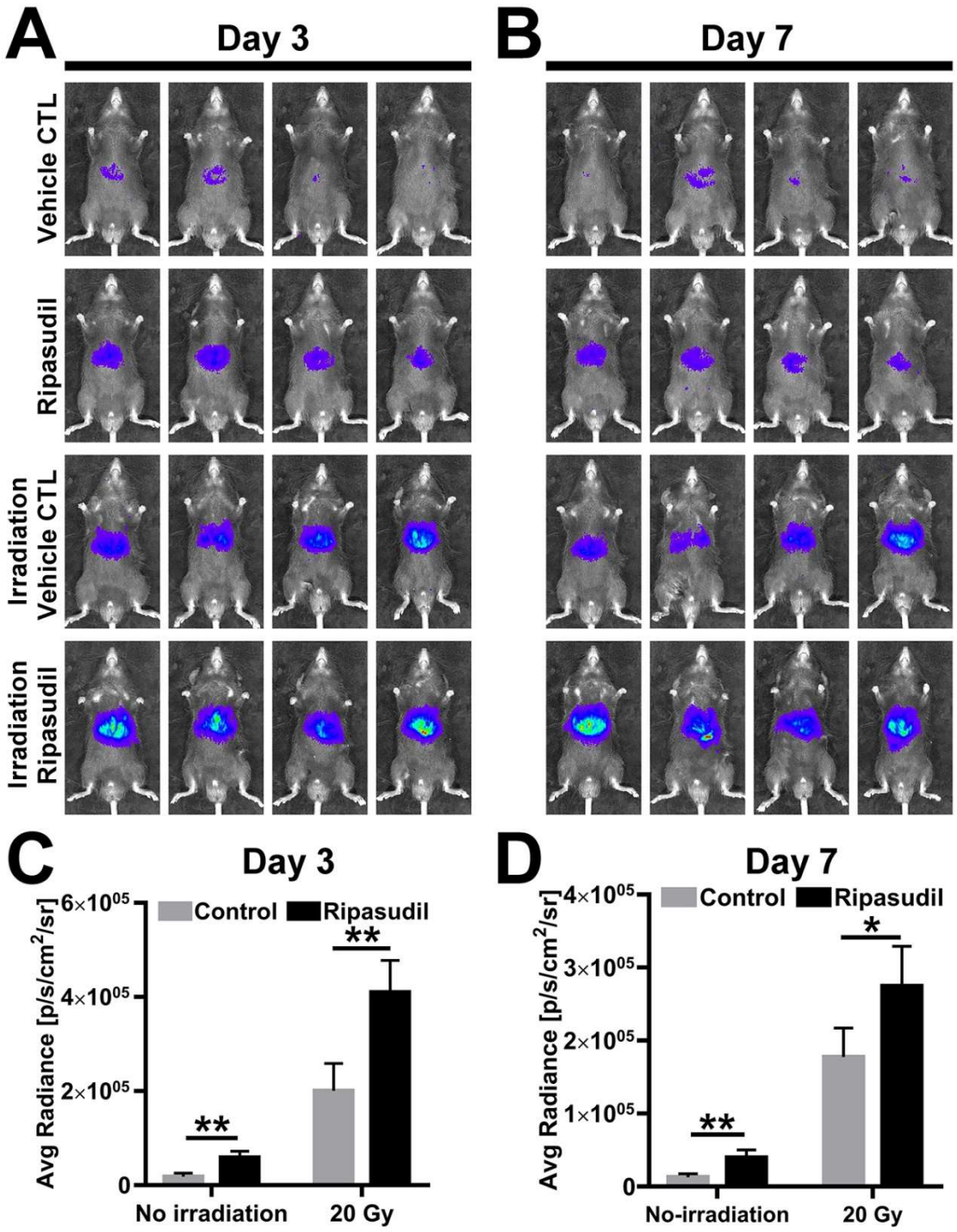

Figure S11. The engraftment of hepatocytes was analyzed by bioluminescence imaging in mice preconditioned with hepatic irradiation and treated with ripasudil. The mice were analyzed at 3 days and 7 days after transplantation. Data are shown as the means ± SEMs (n=4). *p < 0.05. ** P<0.01.

Table S1. shRNA sequences.

shRNA	Hairpin sequence (5'-3')
CD59a shRNA1	CACCGCGGTGGTTTCTTCATGCAATACTCGAGTATTGC ATGAAGAAACCACCGTTTTTT
CD59a shRNA2	CACCGTTGTCATGGTGAGATCATTATCTCGAGATAATGA TCTCACCATGACAATTTTTT
CD59a shRNA3	CACCGCCAGGATTCCTGTCTCTATTTCAAGAGAATAGAG ACAGGAATCCTGGTTTTTT
Scramble shRNA	CACCGTTCTCCGAACGTGTCACGTTTCAAGAGAACGTG ACACGTTCGGAGAATTTTTT

The target sequences are underlined.

Table S2. Antibodies used in immunocytochemistry, immunohistochemistry and western blot.

Antibodies	Source	Application	Dilution
Anti-E-Cadherin, rat monoclonal antibody	Santa Cruz, sc-59778	immunocytochemistry	200
Anti-DPP4, goat polyclonal antibody	R&D, AF954	immunohistochemistry	0.5 μg/ml
Anti-F4/80, rat monoclonal antibody	Santa Cruz, sc-52664	Immunocytochemistry/ immunohistochemistry	200
Anti-CD59a, rabbit monoclonal antibody	Sino Biological, 50724-R108	immunocytochemistry	200
Anti-C5b-9, mouse monoclonal antibody	Santa Cruz, sc-66190	Immunocytochemistry/ immunohistochemistry	200
Anti-E-Cadherin, rabbit monoclonal antibody	Cell Signaling Technology, 3195S	western blot	1000
Anti-CD59, rat monoclonal antibody	Santa Cruz, sc-59095	western blot	500
Anti-GAPDH, mouse monoclonal antibody	Proteintech, 60004-1-Ig	western blot	20000
Anti-β-Actin, HRP-conjugated monoclonal antibody	Proteintech, HRP-60008	western blot	2000

Table S3. PCR primers used in qRT–PCR experiments.

Genes	Forward (5’-3’)	Reverse (5’-3’)
Gapdh	TGGCAAAGTGGAGATTGTTGCC	AAGATGGTGATGGGCTTCCCG
CD59a	TCAATCTGGCTGGGGATGTG	TGAGGCTAACAGCTGTGGAA